AD-A095 507 MICHIGAN UNIV ANN ARBOR F/G 4/1
ABOUT THE PARAMETRIC INTERPLAY BETWEEN IONIC MACH NUMBER, BODY---ETC(U)
DEC 80 U SAMIR, P J WILDMAN, F RICH F19628-79-C-0060
UNCLASSIFIED AFGL-TR-80-0329 NL

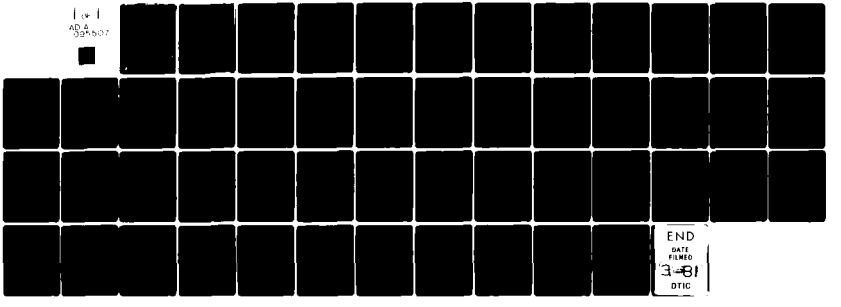

AFGL-TR-80-0329

ABOUT THE PARAMETRIC INTERPLAY BETWEEN IONIC MACH NUMBER, BODY-SIZE AND SATELLITE POTENTIAL IN DETERMINING THE ION DEPLETION IN THE WAKE OF THE S3-2 SATELLITE.

Uri/Samir
P.J.Wildman
F./Rich
H.C.Brinton
R.C.Sagalyn

The Regents of the University of Michigan
218 Research Administration Building
Ann Arbor, Michigan 48109

Final Report, 15 Jan 79 - 30 Sep 80,

Dec 80

50

F19628-79-C-0060

7661

08

Approved for public release; distribution unlimited

AIR FORCE GEOPHYSICS LABORATORY
AIR FORCE SYSTEMS COMMAND
UNITED STATES AIR FORCE
HANSCOM AFB, MASSACHUSETTS 01731

SECURITY CLASSIFICATION OF THIS PAGE (When Data Entered)

REPORT DOCUMENTATION PAGE	READ INSTRUCTIONS BEFORE COMPLETING FORM
1. REPORT NUMBER: AFGL-TR-80-0329 / 2. GOVT ACCESSION NO.: AD-A095 507	3. RECIPIENT'S CATALOG NUMBER:
4. TITLE (and Subtitle): ABOUT THE PARAMETRIC INTERPLAY BETWEEN IONIC MACH NUMBER, BODY-SIZE AND SATELLITE POTENTIAL IN DETERMINING THE ION DEPLETION IN THE WAKE OF THE S3-2 SATELLITE	5. TYPE OF REPORT & PERIOD COVERED: Final Report 15 Jan 1979 - 30 Sept 1980 6. PERFORMING ORG. REPORT NUMBER:
7. AUTHOR(s): Uri Samir *, P. J. Wildman *, F. Rich**, H. C. Brinton***, R. C. Sagalyn*	8. CONTRACT OR GRANT NUMBER(s): F19628-79-C-0060
9. PERFORMING ORGANIZATION NAME AND ADDRESS: The Regents of the University of Michigan, 218 Research Administration Building, Ann Arbor, Michigan 48109	10. PROGRAM ELEMENT, PROJECT, TASK AREA & WORK UNIT NUMBERS: 62101F, 766108AD
11. CONTROLLING OFFICE NAME AND ADDRESS: Air Force Geophysics Laboratory, Hanscom AFB, Massachusetts, Monitor/Irving Michael/PHG	12. REPORT DATE: December 1980 13. NUMBER OF PAGES:
14. MONITORING AGENCY NAME & ADDRESS(if different from Controlling Office)	15. SECURITY CLASS. (of this report): Unclassified 15a. DECLASSIFICATION/DOWNGRADING SCHEDULE:

16. DISTRIBUTION STATEMENT (of this Report)

Approved for public release; distribution unlimited

17. DISTRIBUTION STATEMENT (of the abstract entered in Block 20, if different from Report)

18. SUPPLEMENTARY NOTES

*Air Force Geophysics Laboratory, Hanscom AFB, MA 01731
**Regis College, Research Center, Weston, MA 02193
***NASA Goddard Space Flight Center, Greenbelt, MD 20771

19. KEY WORDS (Continue on reverse side if necessary and identify by block number)

Satellite wakes; influence of Mach number, body potential, body radius, and ion composition on measured current distribution in the wake.

20. ABSTRACT (Continue on reverse side if necessary and identify by block number)

Measurements of ion current, electron temperature and density and values of satellite potential from the U.S.Air Force Satellite S3-2 together with ion composition measurements from the Atmosphere Explorer (AE-E) satellite were used to examine the variation of the ratio $\alpha = \frac{I_+(\text{wake})}{I_+(\text{ambient})}$ (where: I_+ - ion current) with altitude and to examine the significance of the

DD FORM 1 JAN 73 1473

SECURITY CLASSIFICATION OF THIS PAGE (When Data Entered)

Abstract (continued)

parametric interplay between ionic Mach number, normalized body size R_D ($=R_o/\lambda_D$ where: R_o = satellite radius, λ_D = ambient debye length) and normalized body potential ϕ_N($= \frac{e\phi s}{KTe}$ where: ϕ_s = satellite potential, T_e = electron temperature, e and K - constants). It was possible to separate between the significance of R_D and ϕ_N on α. Uncertainty, however, remains regarding the competition between R_D and $S(H^+)$ and $S(O^+)$ (where: $S(O^+)$ and $S(H^+)$ = oxygen and hydrogen ionic Mach numbers respectively) in determining the ion distribution in the nearest vicinity to the satellite surface. A brief discussion is also given regarding future experiments in the area of body-plasma flow interactions to be conducted on board the Shuttle/Spacelab facility.

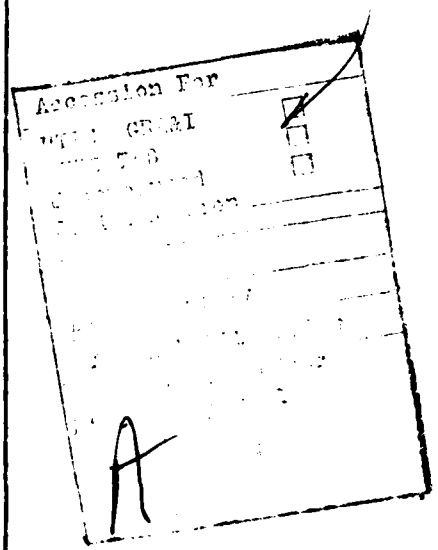

I. Introduction

The motion of a satellite through the terrestrial ionosphere creates disturbances whose spatial extend and temporal characteristics are not yet quantitatively known. Neither are the processes (e.g. particle acceleration, instabilities, wave excitation) acting in the wake zone behind the satellite understood in terms of varying plasma flow and body parameters.

While there is an awareness that such disturbances may have an impact on the reliability of low-energy particle measurements, we find that most published data (from in-situ observations) relating to such disturbances are by-products of geophysical measurements and that no satellite mission had such a study as a major experimental objective. Hence, the available information is fragmentary and does not always lend itself to physically meaningful parametric investigation and/or theory-experiment comparisons.

Theoretical investigations of the effects which occur in the near and far vicinity of spacecraft moving in planetary ionospheres require the self-consistent solution of the Boltzmann-Poisson or the Vlasov-Poisson (for a collisionless plasma) equations under boundary conditions specified by both spacecraft and plasma properties. This is not an easy problem. Therefore, in order to make the mathematical treatment more tractable, simplifying assumptions are used, whose validity and physical significance in determining the overall flow field around the spacecraft are not yet clear. A discussion of various aspects of the problem including those specific cases which lend themselves to semi-analytical treatment is given in Al'pert, 1976. A discussion of theoretical work dealing with various numerical methods and approaches is given by Parker [1976, 1977]. Briefly, among the deficiencies of available theoretical models is the use of linearization procedures which require the plasma potential of the disturbed regions around the spacecraft to be small and solutions are sought at large distances from the spacecraft (where the geometry and size of the body and

sometimes its potential are less significant). In other models the positive ions are treated as neutral particles (i.e., the "neutral approximation") thus, ignoring the effect of electric fields on the ion trajectories. Another major deficiency of present day theories is that the non-stationary case has not been realistically addressed. For discussions on various aspects of the problem, see Al'pert [1976]; Liu [1975a]; Gurevich and Pitaevskii [1975]; Gurevich and Dimant [1975]; Gurevich et al. [1973, 1968, 1966]. In other words, despite the fact that wave excitation and plasma instability in the vicinity of a moving body seem to exist, [Samir and Willmore, 1965; Samir and Wrenn, 1969; Gurevich et al., 1973; Liu, 1975b; Al'pert, 1976], no detailed studies on this basic aspect of the problem have been performed. The latter is surprising in view of the potential application of this area of research to Astrophysics.

Experimental tests of assumptions used in various wake models are practically complicated since most of the available in-situ measurements were made by flush-mounted probes, hence the measurements are confined to the very near vicinity of the bodies. The results presented in this paper are subject to the same limitation. Since the self-consistent numerical solution to the problem of body-plasma interaction (for realistic situations in space) is difficult, it seems that parametric and theory-experiment investigation, limited and imperfect as they may be, can contribute significantly to a better physical understanding of the interactions. The present investigation is aimed at presenting and discussing some experimental results which are useful to some scientific aspects of satellite-ionosphere interactions, as well as to technological/application aspects. In particular to the planning of future experiments of body-plasma electrodynamic interactions in a supersonic and subAlfvenic flow regime to be conducted on board the Shuttle/Spacelab and via the utilization of subsatellites and tethered bodies. More specifically, it is expected that investigations of

the kind presented here be useful: (1) in the planning of instrument location on ejectable ensembles of probes and on the orbiter itself in future shuttle missions, (2) in predicting the disturbances expected to be created by deployed tethered-balloons and other boom-mounted bodies in future shuttle missions and (3) in testing theoretical wake models.

One of the quantities that can serve as a measure of the degree of disturbance produced by the spacecraft motion is the ratio $\alpha = [\frac{I_+(\text{wake})}{I_{+(\text{ambient})}}]$. Unfortunately, there is little systematic experimental information regarding the dependence of α on basic plasma parameters such as: $R_D = (\frac{R_o}{\lambda_D})$; $\phi_N = (\frac{e\phi_s}{KT_e})$; $S = (\frac{V_s}{\sqrt{\frac{2KT_e}{M_+}}})$ and (T_e/T_+) where: R_o = satellite radius, λ_D = Debye length, ϕ_s = satellite potential, T_e = electron temperature, T_i = ion temperature, V_s = satellite velocity, M_+ = ionic mass, K = Boltzmann's constant, e = electronic charge.

It is the major objective of the present investigation to contribute to our knowledge and understanding of the variation of α with some plasma and body parameters.

II. Experimental - The Instruments Used

In order to assess the relative influence of the parameters S, R_D and ϕ_N on the amount of ion depletion in the wake of the S3-2 satellite, measurements of ion current (I_+) electron temperature (T_e), electron density (N_e) and values of plasma potential (ϕ_s) from the planar multigrid probes and from a spherical gridded probe were used. The planar ion probes (or sensors) were flush-mounted on the surface of the satellite and the spherical electron probe was mounted at the end of a boom 1.3 m long and parallel with the satellite spin axis. The ion probes were actually contained in two packages placed 180° apart and with centerlines in the spin plane of the satellite. Each package contains four independent planar ion sensors. Two of these sensors view in the spin plane of the satellite, and two look at 40° on either side of the spin plane. The principal objective of the sensor geometry was to determine direction of bulk ion flow relative to the spacecraft when the sensor array is close to the 'ram' direction. However the 'ram' current flowing to the sensors, together with current measured at other points in the satellite rotation may be used to help build a picture of the positive ion distribution around the satellite. The location of the planar ion-probes on the satellite as well as the location of the electron probe is shown schematically in Figure 1 (a and b). Details of the ion-probe internal configuration, electronics, probe materials and a discussion on probe performance is given in Wildman [1977]. A detailed discussion on the instrument package on the S3-2 satellite is given in Wildman [1976] and Lai et al. [1976], and will not be further discussed here.

If $\alpha = f(R_D)$ at $R_D \approx 40$ (from Figure 4) depicts the behavior of α due to R_D and not due to an $[O^+]$ to $[H^+]$ transition (which happened to occur at the same altitude) than it is possible that the behavior of $\alpha = f(R_D)$ for $R_D \geq 40$ signifies the behavior due to the 'large-body' case [e.g. Al'pert, 1965; Call, 1969; Liu, 1969; Parker, 1976; Al'pert, 1976] where a significant drop in α is expected to occur very close to the satellite's surface. At this point it is not unreasonable to interpret the variation in α including the abrupt drop in terms of $\alpha = f(R_D)$ mainly. However the possibility that this interpretation is not unique exists, e.g. there could have been an $[O^+]$ to $[H^+]$ transition at $H \approx 500$ km. The measurements from the S3-2 satellite could not have revealed such a transition, since no ionic composition measurements were available to us. Figure 5 shows the variation of $\alpha = f(R_D)$ for $25 \leq R_D \leq 56$. As could have been expected [e.g. Samir et al., 1976] α attains an exponentially decreasing value for increasing values of R_D.

Using S3-2 data we have examined $\alpha = f(\phi_N)$ for $|\phi_N|$ in the range $10 < |\phi_N| < 18$. The results are shown in Figure 6. As seen, no obvious correlation between the abrupt change in $\alpha = f(H)$ can be attached to the $\alpha = f(\phi_N)$ variation. In fact, as seen from this figure, significantly different values of α are obtained for the same value of ϕ_N which may imply a behavior due to the influence of another parameter. Examination of the results shown in Figure 5 show that lower values of α correspond to higher values of R_D and higher values of α correspond to lower values of R_D for similar values of ϕ_N. This may suggest that very close to the satellite surface, R_D dominates α more than does ϕ_N.

As mentioned earlier we have attempted to assess the relative importance of S_{AV} in determining the ion distribution in the very near wake and examine the importance of S_{AV} vis-a-vis that of R_D. In carrying out a traditional analysis and using data for [M+(average)] from the literature [e.g. Banks and Kockarts, 1973; Al'pert, 1973] we could find no obvious abrupt change in S_{AV} that could be

correlated with $\alpha = f(H)$ at about 500 km. The change in S_{AV} is being rather gradual.

Since no local ion composition measurements from the S3-2 satellite were available we have attempted to use ion measurements from another satellite with orbits close enough to the ones we used from the S3-2 satellite. It appeared that some orbits of the Atmosphere Explorer E (AE-E) satellite could be considered for this purpose. Therefore, we have examined a fairly large sample of ion composition measurements from the Bennett ion mass spectrometer (BIMS) mounted on board the AE-E satellite.

The mode of operation, technique and method used in the BIMS experiment are given in detail elsewhere [Brinton et al., 1973] and will not be discussed here. Figure 7 shows an example of the final format of the measurements we obtained from the BIMS experiment. In this figure the detailed variation of $[O^+]$, $[H^+]$, $[N^+]$, $[He^+]$ densities with altitude are shown. From such information the transition altitudes of $[O^+]$ to $[H^+]$ is readily obtained. In fact the results of $[N(O^+), N(H^+), N(N^+), N(H_e^+)] = f(H)$ shown in Figure 7 are from the closest orbits we could match to the S3-2 orbit whose $\alpha = f(H)$ results are given in Figure 3. It should be realized that matching 'similar' orbits for the S3-2 and the AE-E satellite is subject to limitations. This is due to the fact that in almost no case could we reach a situation where good coverage of 'overlapping' orbits was possible. For example, latitude could be matched to within (20-25°), longitudes had a wide diversity and local time could be matched to within (3-5) hours difference or more. Figure 7 depicts as reasonable a match as possible between AE-E ion composition results and those shown in Figure 3 for S3-2 results. As seen from Figure 7 a difference of $H \simeq 150$ km exist between the $[O^+]$ to $[H^+]$ transition altitudes for the two orbits shown.

It was interesting to determine the ratio of normalized densities $[\frac{N(\theta)}{N_o}]$ where: N_o = is the ambient density and $90° \leq \theta \leq 180°$ at the $[O^+]$ to $[H^+]$ transition altitude where $N(O^+) = N(H^+)$ and then see where does the value of these ratios fall on the $\alpha = f(H)$ plots e.g. Figure 3. For $[N(\theta)/N_o)]$ we have used expression (1) given below.

$$\frac{N(\theta)}{N_o} = n(O^+) \left[\frac{1+\text{erf}[S(O^+)\cdot K\cdot\cos\theta]}{1+\text{erf}[S(O^+)\ K]}\right] + n(H^+)\left[\frac{1+\text{erf}[S(H^+)K\cdot\cos\theta]}{1+\text{erf}[S(H^+)\ K]}\right] \qquad (1)$$

In this expression [after: Gurevich et al., 1970; Al'pert, 1976] K is a constant ($\simeq 0.6$), θ = angle of attack, $N(\theta)$ = density at the angle θ, N_o = ambient density, $n(O^+)$ and $n(H^+)$ = relative concentration of the $[O^+]$ and $[H^+]$ ions in the plasma and $S(O^+)$ and $S(H^+)$ = corresponding ionic Mach numbers considered separately. In fact, in obtaining expression (1) the two ion species are considered non-interacting and the influence of the electric field upon ion trajectories small. Somewhat more detailed discussions on the latter are given in the Appendix.

In computing $[\frac{N(\theta)}{N_o}]$ we have used the ion measurements from the BIMS experiment [Brinton et al., 1973] on the AE-E satellite with electron temperature measurements from the spherical probe on the S3-2 satellite. We found that the values of $\frac{N(\theta)}{N_o}$ having ratios similar to α occur sometimes close to the altitude where the abrupt drop in α occurs and sometimes at altitudes faraway (by hundreds) of kms) from this altitude. Indeed by comparing $[\frac{N(\theta)}{N_o}]$ values with $[\frac{I(\theta)}{I_o}]$ values we impose a limitation on the study, and this subject was discussed in detail in Samir et al. [1979a] and Samir et al. [1980]. At this point and despite our extensive effort we cannot claim that we have separated between effects due to R_D and those possibly due to the transition of $[O^+]$ to $[H^+]$. On the other hand we have observed that rather than using the parameter S_{AV} it is more useful and realistic to use actual $[M_+(\text{specific})]$ values together with specific T_e values. This is in accord with Samir et al. [1979b] and with the discussion given in

Al'pert [1976] and Gurevich and Pitaevskii [1975] regarding the importance of percentage $[H^+]$ in determining the ion and electron distribution in the wake. From other studies [e.g. Samir et al., 1979a; Samir et al., 1980] we know that $\alpha = f(R_D)$ and that $\alpha = f(\frac{N(O^+)}{N(H^+)}, T_e)$ [e.g. Samir et al., 1979b] hence a dependence on both R_D and $S(O^+)$ and $S(H^+)$ does exist. On the other hand the use of 'average' parameters (e.g. S_{AV}) should be exercised with care and reservation depending on the main objective of the study. For example the S_{AV} is more influenced by the $[O^+]$ ions than by $[H^+]$ ions having the same density. The latter will have a similar influence on S_{AV} as will $[N^+]$ ions having a density which is one order of magnitude less than the $[H^+]$ density.

It is possible that in the very near wake the parameter $R_D = f(T_e, N_e)$ competes with the specific ionic Mach number (S) rather than with $[M_+(\text{average})]$ or S_{AV}. That α is indeed a function of R_D has been shown in Samir et al. [1979a], Samir [1980] and the relationship $\alpha = f(R_D)$ was shown to be exponential for $R_D \geq$ (40-50). Most of the results dealt with in the above papers were confined to altitudes which are below the $[O^+]$ to $[H^+]$ transition with the possible exception of case #4 [Table 2 in Samir et al., 1979a]. And indeed in analyzing the above case the possible contribution of $[N(H^+)/N(O^+)]$ was mentioned.

From the present study it is obvious that more parametric investigations are needed in order to clarify in a more quantitative manner the parametric interplay which determines the ion distribution around the satellite. Such studies are also directly relevant to the determination of the surface of the potential on bodies in space [e.g. Whipple, 1977].

IV. Summary

The variation of ion current depletion in the wake of the S3-2 satellite with altitude in the range 300 km to 1100 km was quantitatively determined. An abrupt drop in ion distribution at about 500 km can be correlated with either a significant change in R_D and/or with a transition between $[O^+]$ to $[H^+]$ or with a combination of both. The relative importance of the parameter $_N$, versus R_D in determining the ion distribution in the wake was examined quantitatively in the range: $10 < |\phi_N| < 18$.

Parametric studies such as attempted here should be continued on board the Spacelab/Orbiter if we are to uniquely resolve the intricacies of the parametric interplay in body-plasma interactions, in supersonic and subAlvenic flow regimes.

Acknowledgement

This work was supported by the U.S. Air Force contract F19628-79-C-0060. We thank Dr. Irving Michael from the Air Force Geophysics Laboratory and Mr. John Metzger from the Space Physics Research Laboratory, University of Michigan for their help in handling S3-2 and AE-E data.

References

Al'pert, Y. L., A. V. Gurevich, and L. P. Pitaevskii, Space physics with artificial satellites, Monography, Consultant Bureau, 1965.

Al'pert, Y. L., Radio wave propagation and the ionosphere, The Ionosphere, Vol. 1, Consultant Bureau, 1973.

Al'pert, Y. L., Wave-like phenomena in the near earth plasma and interactions with man-made bodies, Handbuch der Physik (ed. S. Flugge) Geophysics III, Part V, 217, 1976.

Banks, P. M., and G. Kockarts, Aeronomy, Academic Press, 1973.

Banks, P. M., R. W. Schunk, and W. J. Raitt, The topside ionosphere: a region of dynamic transition, Annual review of earth and planetary sciences, 4, 381, 1976.

Brinton, H. E., H. G. Mayr, R. A. Pickett, and H. A. Taylor, Jr., The effect of atmospheric wind on the O^+-H^+ transition level, Space Res. X, 652, 1970.

Brinton, H. C., L. R. Scott, M. W. Pharo, and J. T. C. Coulson, The Bennett ion-mass spectrometer on Atmosphere Explorer C and E, Radio Sci., 8, 323, 1973.

Call, S. M., The interaction of a satellite with the ionosphere, Report No. 46, Plasma Laboratory, Columbia Univ., 1969.

Gurevich, A. V., L. V. Pariiskaya, and L. P. Pitaevskii, Self-similar motion of rarefied plasma I, Soviet Physics/JETP, 22(2), 449, 1966.

Gurevich, A. V., L. V. Pariiskaya, and L. P. Pitaevskii, Self-similar motion of a low density plasma II, Soviet Physics/JETP, 27(3), 476, 1968.

Gurevich, A. V., L. P. Pitaevskii, and V. V. Smirnova, Ionospheric aerodynamics, Soviet Physics - Uspekhi, 99, (1-2), 595, 1970.

Gurevich, A. V., L. V. Pariiskaya, and L. P. Pitaevskii, Ion acceleration upon expansion of a rarefied plasma, Soviet Physics/JETP, 36(2), 274, 1973.

Gurevich, A. V., and Ya. S. Dimant, Flow of a rarefied plasma around a disc, Geomag. and Aeron., 183, 1975.

Gurevich, A. V., and L. P. Pitaevskii, Non-linear dynamics of a rarefied ionized gas, Prog. Aerospace Sci., 16, 227, 1975.

Lai, S. T., M. Smiddy, and P. J. L. Wildman, Satellite sensing of low energy plasma bulk motion, 7th Conference on Aerospace and Aeronautical Meteorology and Symposium on Remote Sensing from Satellites, November 16-19, 1976.

Liu, V. C., Ionospheric gas dynamics of satellites and diagnostic probes, Space Sci. Rev., 9, 423, 1969.

Liu, V. C., On ionospheric aerodynamics, Prog. Aerospace Sci., 16, 273, 1975a.

Liu, V. C., A wave model of near wakes, Geophys. Res. Lett., 2, 485, 1975b.

Parker, L. W., Computation of collisionless steady-state plasma flow past a charged disc, Report, NASA CR-144159, February 1976.

Parker, L. W., Calculation of sheath and wake structure about a pillbox-shaped spacecraft in a flowing plasma, Proc. Spacecraft Charging Technology Conference (ed. C. P. Pike and R. R. Lovell) p. 331, 1977.

Samir, U., and A. P. Willmore, The distribution of charged particles near a moving spacecraft, Planet. Space Sci., 13, 285, 1965.

Samir, U., and G. L. Wrenn, The dependence of charge and potential distribution around a spacecraft on ionic composition, Planet. Space Sci., 17, 693, 1969.

Samir, U., E. J. Maier, and B. E. Troy, Jr., The angular distribution of ion flux around an ionospheric satellite, J. Atmos. Terrest. Phys., 35, 513, 1973.

Samir, U., R. Gordon, L. H. Brace, and R. F. Theis, The near wake structure of the Atmosphere Explorer C (AE-C) satellite - a parametric investigation, J. Geophys. Res., 84, 513, 1979a.

Samir, U., L. H. Brace, and H. C. Brinton, About the influence of electron temperature and relative ionic composition on ion depletion in the wake of the AE-C satellite, Geophys. Res. Lett., 6, 101, 1979b.

Samir, U., Y. J. Kaufman, L. H. Brace, and H. C. Brinton, The dependence of ion density in the wake of the AE-C satellite on the ratio of body size to Debye length in an $[O^+]$ - dominated plasma, J. Geophys. Res., 85, 1769, 1980.

Titheridge, J. E., Ion transition heights from topside electron density profiles, Planet. Space Sci., 24, 229, 1976.

Whipple, E. C. Jr., Modeling of spacecraft charging, Proc. of Spacecraft Charging Technology (ed. C. P. Pike and R. R. Lovell), 225, 1977.

Wildman, P. J. L., Studies of low energy plasma motion, Results and a new technique, AFGL-TR-76-0168 Report/Air Force Geophysics Laboratory - Space Science Division, 1976.

Wildman, P. J. L., A low energy ion sensor for space measurements with reduced photo-sensitivity, Space Sci. Inst., 3, 363, 1977.

DIAGRAM OF SATELLITE AND PROBE LOCATION

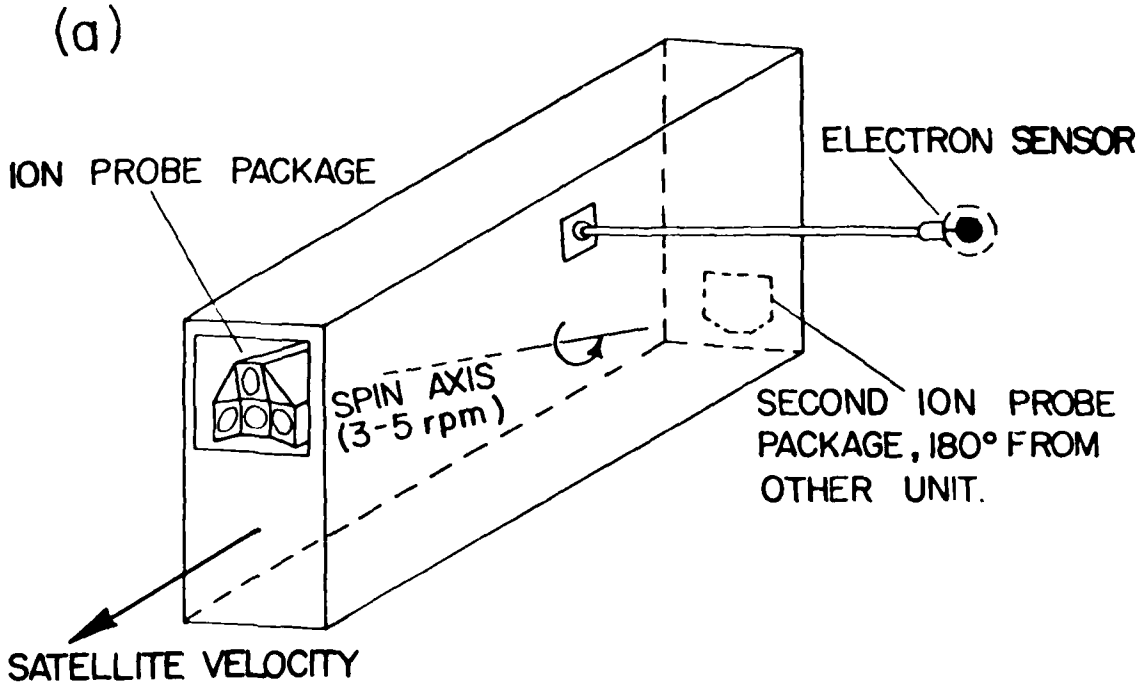

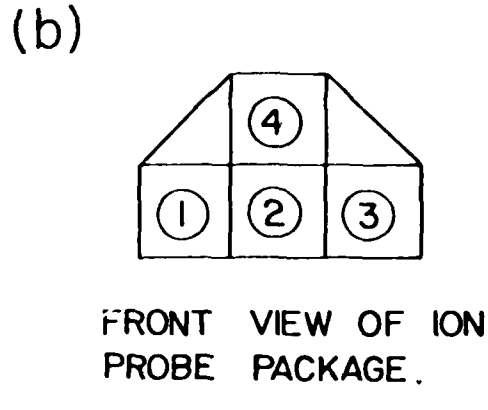

Figure 1: Schematic drawing showing the location of the ion and electron probes on the S3-2 satellite.

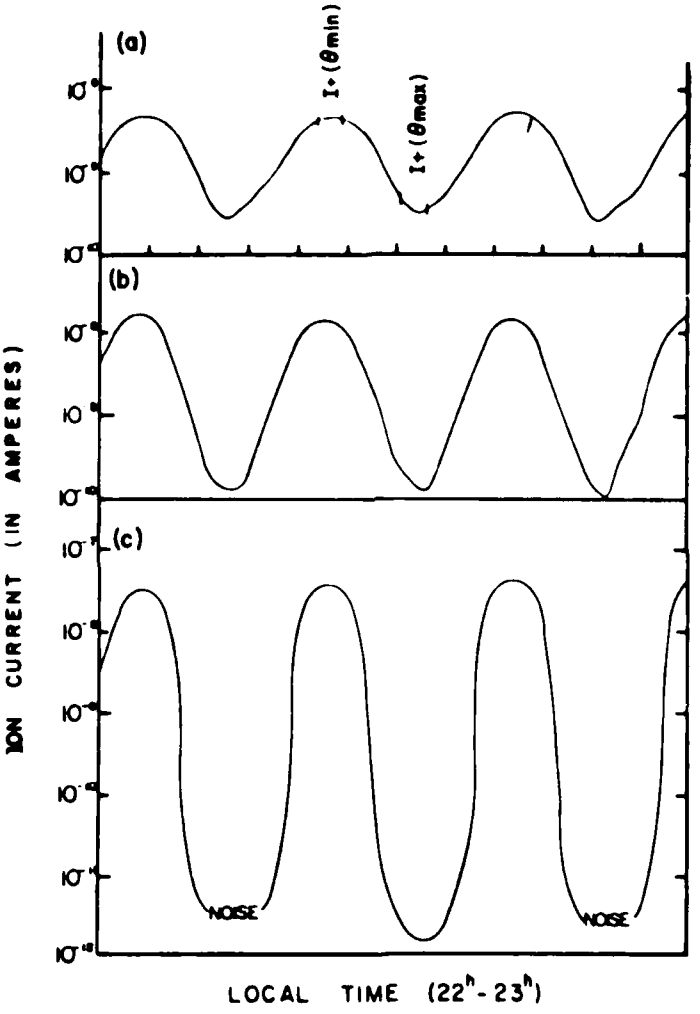

Figure 2: An example showing the general behavior of the ion current with time for the altitude ranges: (a) H = 1094-1056 km, (b) H = 510-477 km, (c) 338-317 km, for equatorial and middle latitudes, at local time $22.5^h \pm 0.5^h$

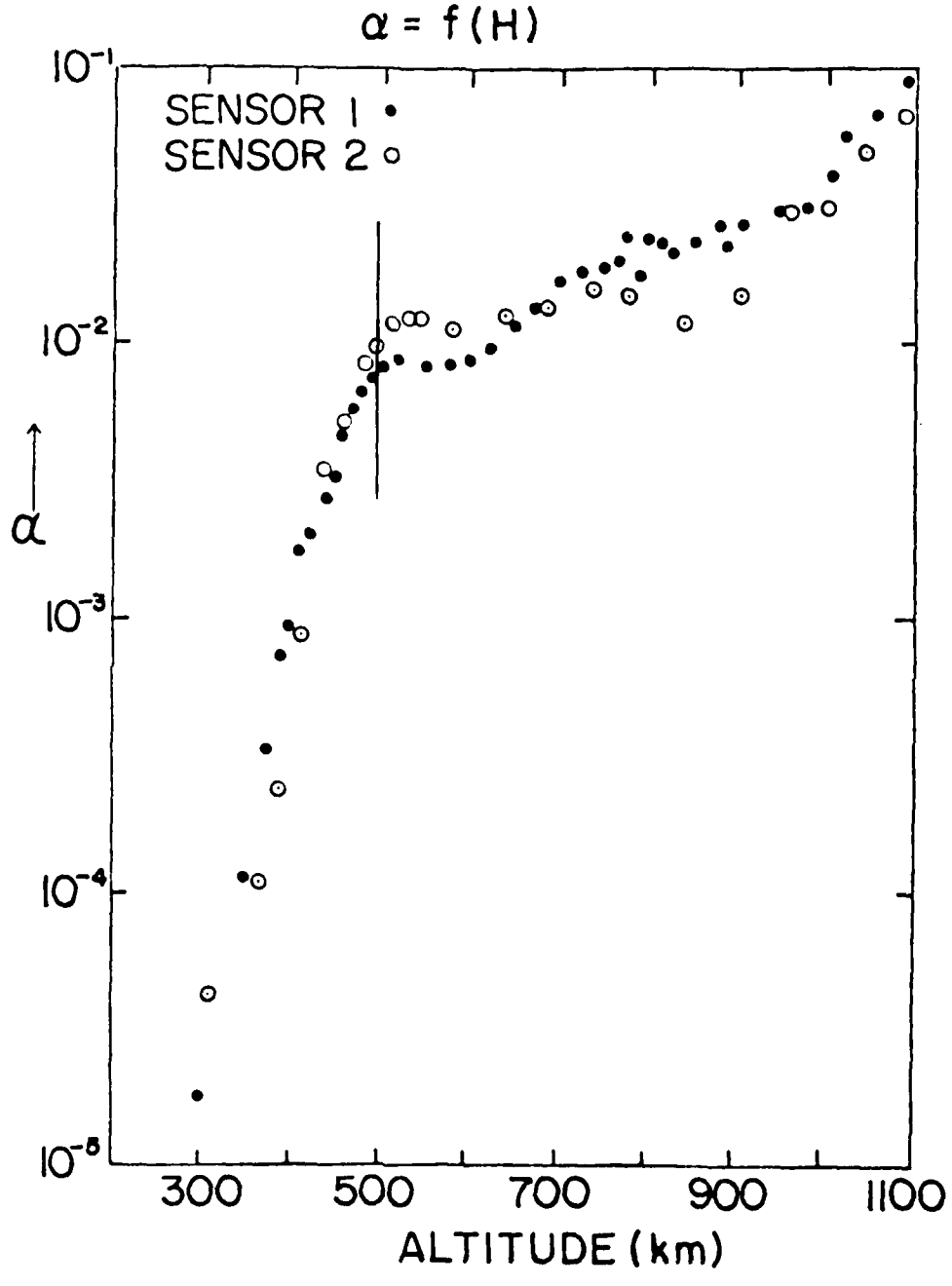

Figure 3: Variation of $\alpha = \left[\frac{I_+(\theta_{max})}{I_+(\theta_{min})}\right]$ with altitude in the range 300 km to 1100 km.

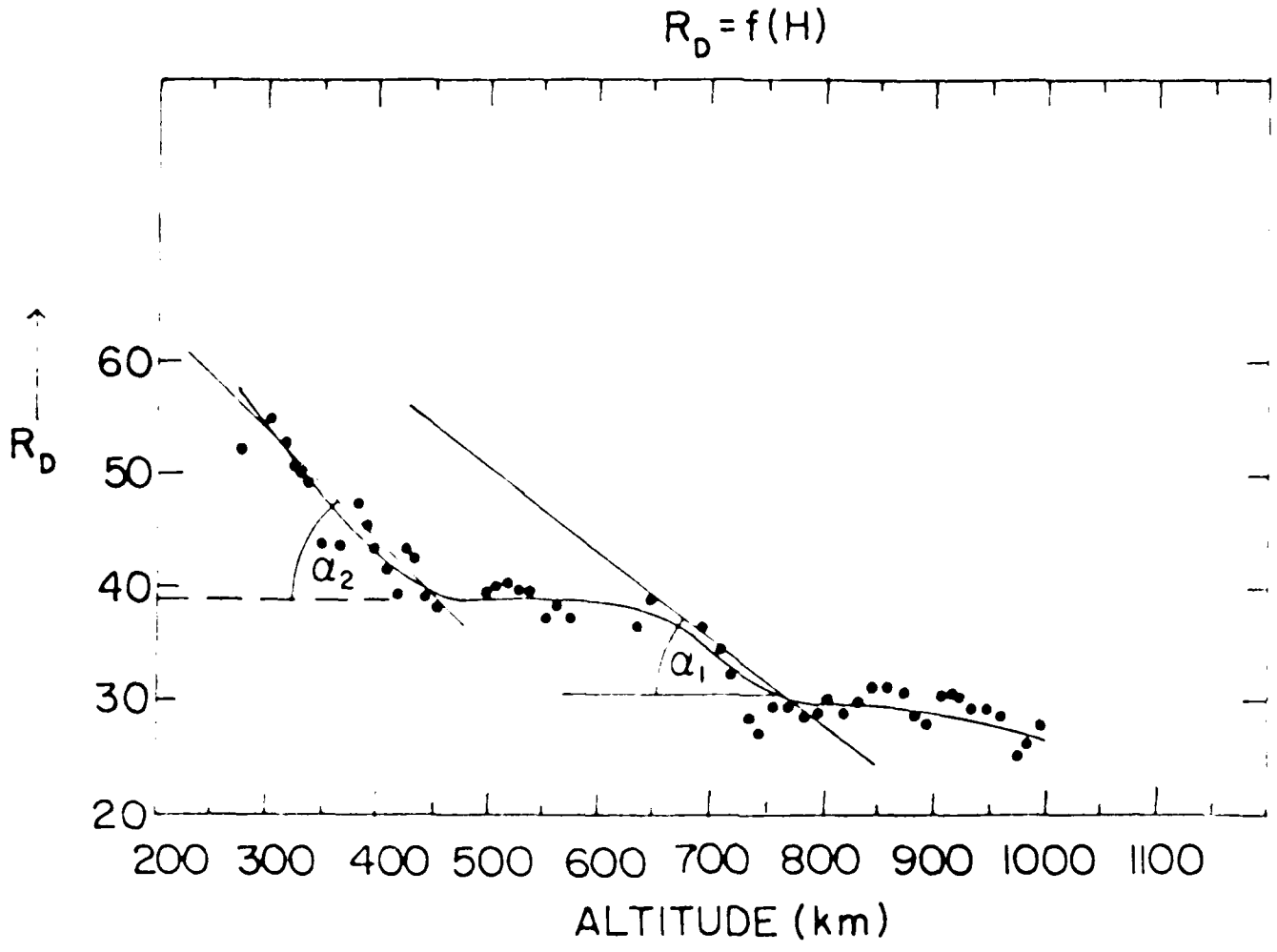

Figure 4: Variation of R_D with altitude in the altitude range: 1000 km to about 300 km.

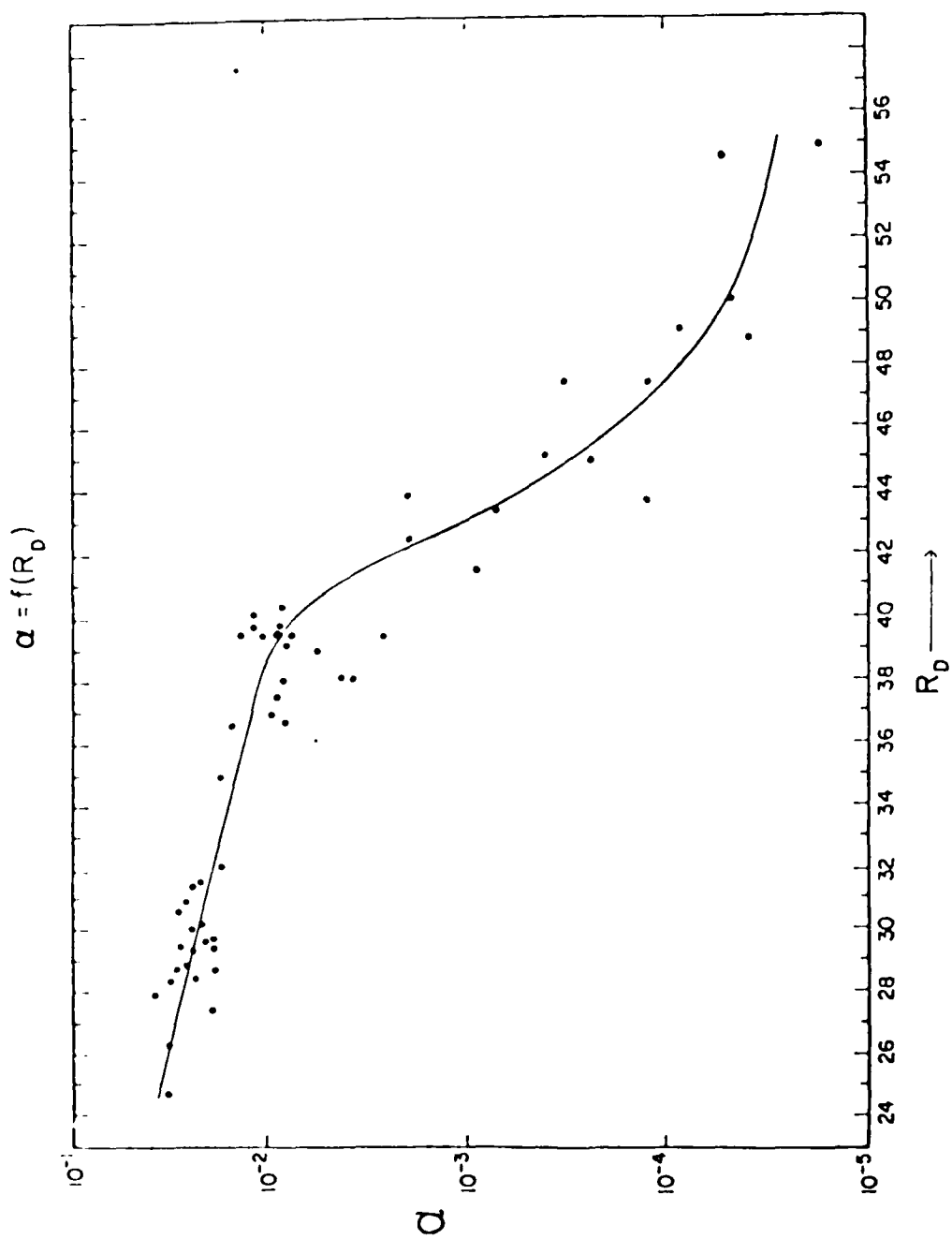

Figure 5: Variation of $\alpha = \left[\frac{I_+(\theta_{max})}{I_+(\theta_{min})}\right]$ with R_D in the range:

$25 < R_D < 56$.

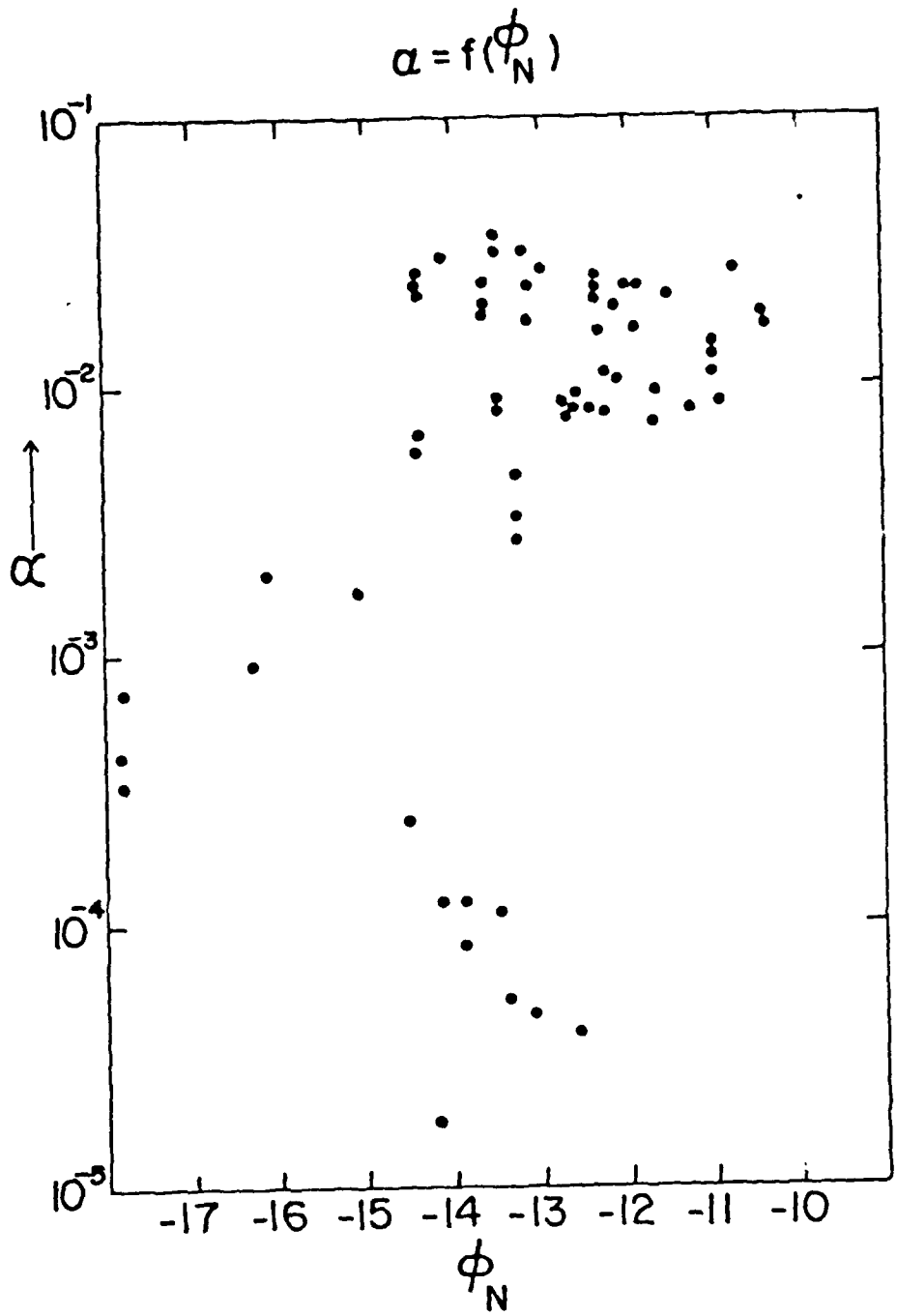

Figure 6: Variation of $\alpha = \left[\frac{I_+(\theta_{max})}{I_+(\theta_{min})}\right]$ with ϕ_N in the range:

$10 < |\phi_N| < 18.$

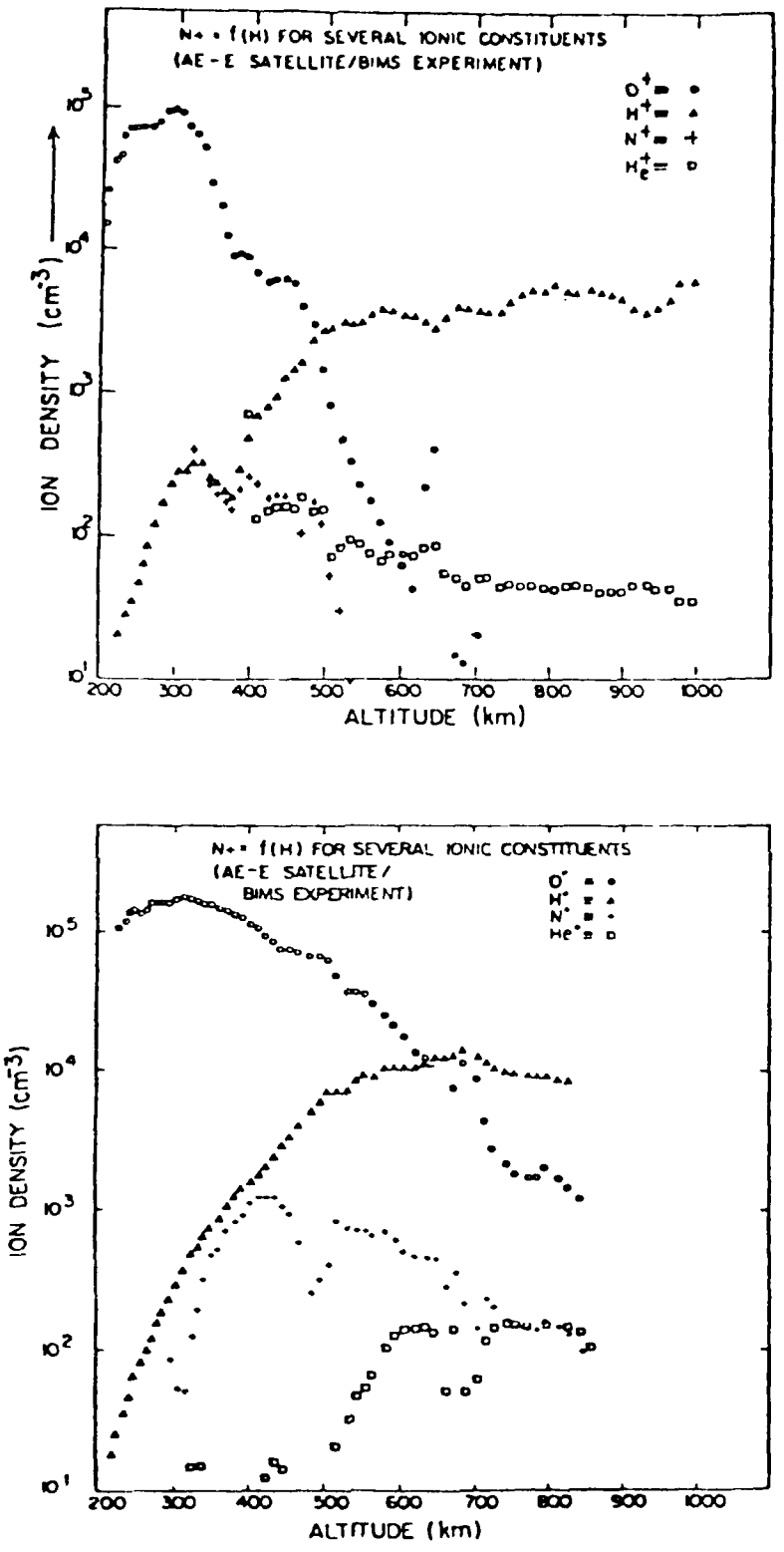

Figure 7: Variation of $N^+ = f(H)$ for several ionic constituents. Measurements from the AE-E Satellite/BIMS experiment.

APPENDIX: ABOUT THE EXPRESSION $[\frac{N(\theta)}{N_o}]$ USED IN THE PAPER*

I. About Bibliography

In the paper (Gurevich and Pitaevskii, 1975) a detailed discussion of non-linear dynamics regarding rarefied ionized gases is given in detail. In Gurevich et al. (1970) and Al'pert (1976) detailed discussions are given regarding the various aspects of the interaction between a rarefied plasma and a supersonically moving body. The latter two references extend studies performed by Gurevich, Pitaevskii, Al'pert and colleagues during the past two decades and are in fact a continuation to Al'pert et al. (1965), which summarized earlier work by the above Russian group.

It is somewhat surprising that while an extensive theoretical effort took place in Russia regarding body-plasma interaction less intensive and meaningful work was performed in the U.S.A. It appears justified to say that many theoretical modeling as well as experimental work regarding 'spacecraft charging' would have benefited significantly if more attention would have been paid to the Russian theoretical work.

In the following sections we deal with some aspects of body-plasma interactions based on Russian work.

II. Assumptions and Basic Equations

A. We first deal with one-dimensional quasi-neutral flows in the absence of a magnetic field.

The basic mathematical approach relies on the analogy to hydrodynamics, in particular to the self-similar solutions which do not contain any characteristic dimensions in the initial and final conditions. Namely, the time t and the coordinate x appear in the solution of such problems only in some combinations of (x/t). It is argued (e.g. Gurevich and Pitaevskii, 1975) that

*The contents of this Appendix is part of a review paper by U. Samir now in preparation.

self-similar solutions in hydrodynamics describe a large class of physical problems among which is the study of the wake behind a body. Therefore it should be of interest to examine the situation for a rarefied plasma described by the collisionless kinetic equation with a self-consistent field.

In this appendix we summarize some of the findings which are relevant to body-plasma interactions in planetary ionospheres and magnetospheres, in particular, the validity of the approach. This will be done via the comparison with in situ experimental results.

Considering the one dimensional case and assuming that at an initial time the plasma occupies the half-space $x < 0$ and then expands into the other half of the space ($x > 0$) then the plasma is described by the kinetic equation for the distribution function for ions:

$$\frac{\partial f}{\partial t} + \frac{\partial f}{\partial x} v - \frac{\partial f}{\partial v}\left(\frac{e}{M}\right)\frac{\partial \varphi}{\partial x} = 0 \tag{1}$$

where M = mass of the ions, ϕ = the electric potential. (Note: A similar equation can be written for the electron distribution function) and by the Poisson equation:

$$\frac{\partial^2 \varphi}{\partial x^2} = -4\pi e\left(N - N_e\right) \tag{2}$$

$$N = N(x,t) = \int_{-\infty}^{+\infty} f\, dv$$

where N = ion number density, N_e = electron density. We also assume that:

$$N_e = N_0 \exp\left(-\frac{e\varphi}{K T_e}\right) \tag{3}$$

i.e., the equilibrium distribution of ions is described by the Boltzmann formula (3). Note: There are other distributions for electrons (e.g. Gurevich and Pitaevskii (1975), p. 258. We now adopt the Russian notation whereby T_e is given in eV, hence

$$\frac{N}{N_0} = \exp\left(\frac{e\varphi}{T}\right) \tag{3}$$

For a quasi-neutral plasma, and the argument is that this is the case for the greater part of the region behind a body (i.e., of the wake) we have:

$$N = N_e \tag{4}$$

and it follows that

$$e\varphi = T \cdot \ln\left(N/N_0\right) \tag{5}$$

which then yields for (1) the equation:

$$\frac{\partial f}{\partial t} + \frac{\partial f}{\partial x} v - \frac{\partial f}{\partial v}\left(\frac{1}{M}\right)\frac{\partial}{\partial x}\left(\ln \int_{-\infty}^{+\infty} f\,dv\right) = 0 \tag{6}$$

Introducing non-dimensional and self-similar quantities:

$$\left.\begin{aligned} \tau &= \sqrt{\frac{M}{2T}}\left(\frac{x}{t}\right) = \left(\frac{x}{t}\right)\left(\frac{M}{2T}\right)^{1/2} \\ g &= \left[\left(\frac{2\pi T}{M}\right)^{1/2} \cdot f\right]/N_0 = \frac{1}{N_0}\left(\frac{2\pi T}{M}\right)^{1/2} \cdot f \\ u &= v\left(\frac{M}{2T}\right)^{1/2} \end{aligned}\right\} \tag{7}$$

We obtain the equation for the ion-distribution function:

$$(u-\tau)\frac{\partial g}{\partial \tau} - \frac{1}{2}\frac{\partial g}{\partial u}\cdot\frac{\partial \psi}{\partial \tau} = 0 \qquad (8)$$

with:
$$\psi = \frac{e\varphi}{T_e} = \ln(n) = \ln\left(N/N_0\right)$$
$$n = \int g \frac{du}{\sqrt{\pi/\beta}} \quad ; \quad \beta = \frac{T_e}{T_i} \qquad (9)$$

For the case $T_e << T_i$, the electrons play a small part. Hence in this case, the last term in equation (1) can be neglected and equation (1) becomes:

$$\frac{\partial f}{\partial t} + v\frac{\partial f}{\partial x} = 0 \qquad (10)$$

And equation (10) is the equation describing a free molecular flow of neutral gas.

This case is thus called the "neutral approximation". The general solution of (10) is:

$$f(x,v,t) = f_0(x-vt, v) \qquad (11)$$

where $f_o(x, v)$ is the initial distribution function.

For the case $T_e >> T_i$ the part played by the electric field becomes very important. To first approximation, the thermal motion of the ions can be neglected ($T_i/T_e \to 0$), hence the distribution function for ions can be represented by a δ-function of velocity, i.e., has the form:

$$f(x,v,t) = N(x,t)\cdot\delta\left(v-\bar{v}(x,t)\right) \qquad (12)$$

Substitution of (12) in (1) yield:

$$\left.\begin{aligned} &\frac{\partial N}{\partial t}+\frac{\partial}{\partial x}\left(N\bar{v}\right)=0 \\ &\frac{\partial \bar{v}}{\partial t}+\bar{v}\frac{\partial \bar{v}}{\partial x}+\left(\frac{e}{m}\right)\frac{\partial \varphi}{\partial x}=0 \\ &\varphi=\left(\frac{T_e}{e}\right)\cdot \ln(n) \end{aligned}\right\} \qquad (13)$$

The eq. (13) coincide with the hydrodynamic equations for an ideal isothermal gas. Note: In Gurevich and Pitaevskii (1975), Appendix III, p. 261 a discussion on the inclusion of the ion thermal motion is given.

In summary: The basic idea in the Russian work discussed above is the possibility of using a self-similar approach i.e., seeking solutions which depend on (x/t) in a way which is analogous to (in some cases) ideal fluids in hydrodynamics. Therefore, non-dimensional variables (e.g. t, g, u) are introduced and cases of interest to space plasma physics are treated in an analogous manner.

B. Discussion of the self-similar method

The basic equations are:

$$\left.\begin{aligned} &(u-\tau)\frac{\partial g}{\partial \tau}-\frac{1}{2}\frac{\partial g}{\partial u}\frac{\partial \psi}{\partial \tau}=0 \\ &\psi=\frac{e\varphi}{T_e}=\ln(n) \\ &n=\int g\,\frac{du}{\sqrt{\pi/\beta}} \quad ; \quad \beta=\frac{T_e}{T_i} \end{aligned}\right\} \qquad (8\text{-}9)$$

In mathematical terms it is possible to discuss the boundary conditions of

$$\left.\begin{aligned} &\frac{\partial f}{\partial t}+v\frac{\partial f}{\partial x}-\left(\frac{T_e}{M}\right)\frac{\partial f}{\partial v}\frac{\partial}{\partial x}\left(\ln n\right)=0 \\ &n=\frac{N}{N_0}=\frac{1}{N_0}\int f\,dv \end{aligned}\right\} \qquad (14)$$

Note: Eq. (14) is essentially the same as (6) in the preceding section.

in terms of a decay of an arbitrary initial discontinuity. Then the boundary conditions for (14) for an arbitrary initial discontinuity are:

$$f(x,v)_{t=0} = \begin{cases} f_1(v) & \text{for } x<0 \\ f_2(v) & \text{for } x>0 \end{cases} \tag{15}$$

where: f_1 and f_2 are arbitrary initial distribution functions of the ions on the left hand side and on the right hand side of the discontinuity. In terms of the non-dimensional variable (T) defined as: $\tau = [\frac{x}{t}(\frac{M}{2T_e})^{\frac{1}{2}}]$ (defined in eq. (7)), we obtain for the distribution functions g_1 and g_2:

$$\left.\begin{aligned} g &= g_1(u) \;;\; \text{for } \tau = -\infty \\ g &= g_2(u) \;;\; \text{for } \tau = +\infty \end{aligned}\right\} \tag{16}$$

And for f_1 and f_2 chosen as Maxwellian functions in the form:

$$\left.\begin{aligned} f_1 &= N_0\left(\frac{M}{2\pi T_i}\right)^{1/2} \exp\left[-\frac{Mv^2}{2T_i}\right] \\ f_2 &= N_0\left(\frac{M}{2\pi T_{i2}}\right)^{1/2} \exp\left[-\frac{M(v-v_0)^2}{2T_{i2}}\right] \end{aligned}\right\} \tag{17}$$

Note: The ions in region I are considered here to be at rest.

Hence for g_1 and g_2 we obtain:

$$\left.\begin{aligned} g_1 &= \exp(-\beta u^2) \\ g_2 &= \left(\frac{N_2}{N_0}\right)\left(\frac{T_i}{T_{i2}}\right)^{1/2} \exp\left[-\beta_2(u-u_0)^2\right] \end{aligned}\right\} \tag{18}$$

where: $u_0 = \left(\frac{Mv_0^2}{2T_e}\right)^{1/2}$; $\beta = \frac{T_e}{T_i}$; $\beta_2 = \frac{T_e}{T_{i2}}$

Equations (8-9) determines g(t, u) via the method of characteristics i.e., considering the curves on which g has a constant value (see Gurevich and Pitaevskii, 1975). The equation of the characteristics is:

$$\frac{du}{d\tau} = \frac{1}{2}\left(\frac{F(\tau)}{u-\tau}\right) \quad ; \quad F(\tau) = -\frac{1}{n}\left(\frac{dn}{d\tau}\right) \tag{19}$$

where $F(\tau)$ is a non-dimensional force acting on the ions which is proportional to the strength of the electric field in the plasma.

In dealing with the character of $n(\tau)$ for the "neutral approximation" case Gurevich and Pitaevskii (1975) show that for the boundary conditions (15) we get:

$$f(x,v,t) = \begin{cases} f_1(v), & \text{for } x < vt \\ f_2(v), & \text{for } x > vt \end{cases}$$

and:

$$n(\tau) = \int_{\tau}^{\infty} g_1(u)\frac{du}{\sqrt{\pi/\beta}} + \int_{-\infty}^{\tau} g_2(u)\frac{du}{\sqrt{\pi/\beta}} \tag{20}$$

The extremium of the function $n(\tau)$ is given by the condition: $[dn/d\tau] = 0$, namely:

$$g_1(\tau) - g_2(\tau) = 0 \tag{21}$$

Now, depending on the relations between No, N_2, T_i, T_{i2}, v_o a distinction should be made for the following three cases:

$$\left.\begin{array}{ll} \text{(i)} & T_i \gg T_{i2} \\ \text{(ii)} & T_i = T_{i2} = T, \quad v_0 \neq 0 \\ \text{(iii)} & T_i = T_{i2} = T, \quad v_0 = 0, \quad N_0 > N \end{array}\right\} \tag{22}$$

These cases are being discussed and the behavior of the distribution function $g = f(u)$ is given for each of the above cases (see Fig. 1, p. 231 in Gurevich and Pitaevskii, 1975). Also, the behavior of the non-dimensional force $F(\tau)$ is given for each of the above cases (see Fig. 2, p. 231 in the above reference). In Summary: It is found that for case (i) we have:

$$g_1(u) \sim \exp\left(-\frac{T_e}{T_i}u^2\right) \gg g_2(u) \sim \exp\left(-\frac{T_e}{T_{i2}}u^2\right) \tag{23}$$

For case (ii) we have:

$$\left.\begin{array}{l} g_1 \sim \exp\left(-\frac{T_e}{T}u^2\right) \\ g_2 \sim \exp\left(-\frac{T_e}{T}u^2\right) \cdot \exp\left(2uu_0\frac{T_e}{T}\right) \end{array}\right\} \tag{24}$$

Note: The above analysis is for the "neutral approximation".

However, with the exception of the case $T_e/T_i \to \infty$ qualitative conclusions are valid not only for the "neutral approximation: situation.

For the asymptotic behavior of the function $(\frac{dn}{d\tau})$ for $\tau \to \pm\infty$, particles with large velocities (u) are most important. And in all cases except for the case of the expansion of a plasma into a vacuum (see curve 2 in Fig. 2c) the jump of the electric potential $|\phi_{x \to -\infty} - \phi_{x \to +\infty}|$ appears to be finite hence the distribution of fast particles does not vary with the field.

Therefore, the asymptotic expressions (23) and (24) remain valid when the electric field is taken into account. Note: This is a very significant conclusion that may be used for pratical cases and simplify the calculations. Furthermore, Gurevich and Pitaevskii (1975) claim that the qualitative con-

siderations concerning the shape of n(t) remain valid. And even for the case where the electric field can change the asymptotic value of the coefficient of $[\exp(-\frac{T_e}{T} u^2)]$ the monotonic behavior of $[n(\tau)]$ does not change.

III. Discussion of Some Relevant Specific Cases

B. The free expansion of a plasma into a vacuum

Here as in the discussion in Section II the problem is dealt with in a self-similar manner (for a collisionless plasma). The density and the velocity distribution of the ions are obtained (Gurevich et al., 1968). The main finding is that in the course of filling the rarefied half-space (e.g. the wake region behind a body) a part of the ions is accelerated by the action of the resulting electric field up to velocities of the order of the thermal velocity of the electrons. At the same time the effective temperature of the ions drops sharply. In fact the drop is such that the effective ion temperature is many times smaller than the electron temperature (for the initial situation of $T_e = T_i$).

Here we will briefly discuss the results of relevance to spacecraft-space-plasma interactions.

Starting with (1) and (2) using (3), (4), (5) equation (6) is obtained. Using the non-dimensional quantities given in (7) equation (8) is obtained. Assuming that for $x < 0$ the plasma is not perturbed, while for $x > 0$ there is no plasma at all (i.e., vacuum) and assuming that for $x < 0$ the plasma is Maxwellian, the boundary conditions for the equation ($8 \equiv 8^*$), i.e., for:

$$(u-\tau)\frac{\partial g}{\partial \tau} - \frac{1}{2}\frac{\partial g}{\partial u}\frac{d}{d\tau}\left(\ln \int_{-\infty}^{+\infty} g\,du\right) = 0 \qquad (8^*)$$

are:

$$\tau \longrightarrow -\infty \;;\; g \longrightarrow \exp(-u^2)$$

$$\tau \longrightarrow +\infty \;;\; g \longrightarrow 0 \qquad (25)$$

First, the asymptotic cases $\frac{T_e}{T_i} \to 0$ and $\frac{T_e}{T_i} \to \infty$ are discussed. The case of $\frac{T_e}{T_i} \to 0$ (or: $\beta = \frac{T_e}{T_i} << 1$): This case is essentially the 'neutral approximation' case discussed in Section II. Hence, expressions (10) and (11) apply here and the distribution function and $n(\tau)$ i.e., the ion concentration distribution are sought from (20) with $g_2 = 0$ (based on (25)). Thus for $n(\tau)$ we obtain:

$$n(\tau) = \frac{1}{\sqrt{\pi}} \int_{\tau}^{\infty} \exp(-u^2)du = \frac{1}{2}\left[1 - erf(\tau)\right] \qquad (26)$$

Now, for $\tau >> 1$ (note that large τ values correspond to large values of x) we obtain:

$$n(\tau) = \left(\frac{1}{2\sqrt{\pi}}\right)\cdot\left(\frac{1}{\tau}\right) \exp(-\tau^2) \qquad (27)$$

Note: Expression (27) represents n(t) for $\tau >> 1$ (or: $\tau \to +\infty$) near the vicinity of the body or plane behind which there was initially a vacuum, and the plasma expanded into.

The Case of $\frac{T_e}{T_i} \to \infty$, (or $\beta = \frac{T_e}{T_i} >> 1$): In this case the thermal velocity of the ions is less than the velocity of the ions which corresponds to the ordered motion (stream velocity) produced by the electric field. In this case (argues: Gurevich et al., 1969) there is no need to use the kinetic equation. For this case the equation for the velocity (v) corresponding to the ordered motion should be adequate. Therefore equations (13) apply here and from which follow:

$$\left.\begin{aligned} &\frac{\partial \bar{u}}{\partial t} + \bar{u}\frac{\partial \bar{u}}{\partial \rho} + \frac{1}{2N}\frac{\partial N}{\partial \rho} = 0 \\ &\frac{\partial N}{\partial t} + \frac{\partial}{\partial \rho}(N\bar{u}) = 0 \;;\; \bar{u} = v_\rho\left(\frac{M}{2T_e}\right)^{1/2} \end{aligned}\right\} \qquad (28)$$

where: $\vec{\rho} = \frac{\vec{r}}{R_o}$ (and for one dimension we are concerned only with x as is the case here).

Finally we obtain from (28):

$$\left.\begin{aligned}(\bar{u}-\tau)\frac{d\bar{u}}{d\tau}+\frac{1}{2N}\frac{dN}{d\tau}&=0\\(\bar{u}-\tau)\frac{dN}{d\tau}+N\frac{d\bar{u}}{d\tau}&=0\end{aligned}\right\} \qquad (29)$$

Again (29) describes the ion motion as does the equation of motion for an isothermal ideal gas (with temperature T_e) in hydrodynamics.

The system of equations (29) has two solutions. One which is trivial i.e., N = const, $\bar{u}$ = const. and the second is:

$$\left.\begin{aligned}(\bar{u}-\tau)^2=\frac{1}{2}\;;\;\bar{u}=\tau+\frac{1}{\sqrt{2}}\\ n(\tau)=\frac{N}{N_0}(\tau)=C\exp\left(-\sqrt{2}\cdot\tau\right)\end{aligned}\right\} \quad \text{for: } \tau\gg 1 \qquad (30)$$

where C is a constant (C ≈ 0.7).

The continuous solution, satisfying (25) for $\tau \to -\infty$ ($N = N_0$, or $n = 1$; $\bar{u} = 0$) and for $\tau \to +\infty$ ($n = 0$) is:

$$\bar{u}=0,\ n=1 \quad at \quad \tau<-\frac{1}{\sqrt{2}}$$

$$\bar{u}=\tau+\frac{1}{\sqrt{2}},\ n=\exp\left(-\sqrt{2}\cdot\tau-1\right) \quad at \quad \tau>-\frac{1}{\sqrt{2}} \qquad (31)$$

And the electric field appearing as a result of the flow has the form:

$$E=\frac{(MT_e)^{1/2}\cdot V_0}{2^{1/2}\cdot e\cdot z}F(\tau) \qquad (32)$$

where:

$$F(\tau)=\begin{cases}0, & \tau<-\frac{1}{\sqrt{2}}\\ \sqrt{2}, & \tau>-\frac{1}{\sqrt{2}}\end{cases}$$

and the basic definition of $F(\tau)$ is:

$$F(\tau)=-\beta\frac{d}{d\tau}\left(\ln\int_{-\infty}^{+\infty}g\,du\right) \qquad (33)$$

It should be realized that the line $\tau = -\frac{1}{\sqrt{2}}$ (see Figure A-3) is the line that separates the region occupied by the gas at rest and the region occupied by the moving gas. The first derivatives of $\bar{u}$ and N have a discontinuity along this line. A discontinuity in the electric field strength means that there is a charged electric layer along this line. This layer is of the order of a Debye length.

An important point to note is that for large values of (t), the expression (31) gives much higher values than those obtained by expression (27). Namely:

$$n \approx \exp\left(-\tau\cdot\sqrt{2}\right) \Bigg\} \quad (34)$$

rather than:

$$n \approx \exp\left(-\tau^2\right) \Bigg\}$$

This result is due to the strong influence of the electric field on the ion motion i.e., due to the acceleration of part of the ions by the electric field.

The general case i.e., any β:

Mathematically, for the general case i.e., (any value of β) one seeks the solution of equations (8-9) namely, the determination of the behavior of the characteristics. This is dealt with in great detail in Gurevich et al. (1969) and Gurevich and Pitaevskii (1975).

Here we will bring only the results of interest to us.

Figure A-4 shows the relation between $n = \frac{N}{N_o}$ plotted as a function of (t) $\left[\tau = \left(\frac{x}{z}\right)\left(\frac{Mv_o^2}{2T_e}\right)^{1/2}\right]$ for various values of $\beta\left(\equiv \frac{T_e}{T_i}\right)$. The dotted line is the case of isothermal hydrodynamics which corresponds to the limit $\beta \to \infty$ (expression (30)). It is seen that with the increase of β the distribution $[n(\tau)]$ approaches the hydrodynamic case given in expression (30).

Figure A-5 depicts the same on a logarithmic scale (for: $\beta = 1$). The dotted line is obtained using the free molecular motion ($\beta \to 0$) i.e., the

heutral approximation' (given in expression (27)).

From Figure A-5 we see that for larger values of t the values of $n(=\frac{N}{N_o})$ decrease slower than do the values of (n) in the 'neutral approximation'. This is due to the influence of the electric field.

The asymptotic behavior of $n(\tau)$ for $\tau >> 1$ is given by (31) namely:

$$n(\tau) \approx C \exp(-\tau\cdot\sqrt{2}) \qquad (35)$$

with C = 0.7 for $\beta = 1$. For arbitrary values of β the 'constant' C is $C(\beta)$ and is given by:

$$C(\beta) = \frac{2\sqrt{\beta}}{\sqrt{3}}\left[\frac{\sqrt{3+\beta}-\sqrt{\beta}}{\sqrt{3+\beta}+\sqrt{\beta}}\right]^{1/2}\cdot\exp\left[\sqrt{1+\frac{3}{\beta}}-2\right] \qquad (36)$$

Figure A-6 shows the distribution function g as a function of u for different values of (τ) and for $\beta = 1$. This is a very important figure since it shows quantitatively how the electric field influences the distribution function of the ions. As seen from this figure, for $\tau << -1$ the function g is an unperturbed Maxwellian. Thus for example for $\tau \approx -2$ the distribution function g is close to $[\exp(-u^2)]$. And in fact for $\tau < 0$ these functions are close enough to the distributions obtained from the "neutral approximation". This however is not the case for large positive values of (τ), or: for $\tau > 1$. Figure A-6 shows the gradual conversion of the Maxwellian distribution function to a δ-type function, i.e., to a needle-type (or: needle-shaped) function is the region of "strong rarefaction" i.e., in the region where $\tau >> 1$ (and: $\tau = \xi/t = \left[\left(\frac{Mv_o^2}{2T_e}\right)^{1/2}\cdot\frac{x}{z}\right]$ where: $t = \left[z\cdot\sqrt{\frac{2T_e}{Mv_o^2}}\right]$.

Again the needle-shaped functions (for increasing values of τ) indicate the strong acceleration of a portion of the ions which fill in the rarefied region.

Moreover, Gurevich et al. (1966) show that the mean energy of the ions for large values of τ is equal to:

$$\mathcal{E} = \frac{1}{2} M_i \bar{v}^2 \approx T \cdot \tau^2 \tag{37}$$

from which follows that the energy of the ions can exceed the initial thermal energy by orders of magnitude. The effect of acceleration can even be larger for a bithermal (e.g. $\beta > 1$; $T_e > T_i$) plasma. Note that this latter case is common in laboratory simulation studies.

Furthermore, Gurevich et al. (1966, 1969) and Gurevich and Pitaevskii (1975) show that as τ increases the thermal velocity spread of the ions diminishes rapidly. And that the quantity: $\left[(T_i)\ effective\right] = 2T[\bar{u} - \bar{u}]$ which has the meaning of an "effective" ion temperature and varies with increasing τ in the form:

$$(T_i)_{effective} \sim T \exp(-2\tau\sqrt{2}) \tag{38}$$

The latter has an important effect on the stability of the region behind a rapidly moving body e.g. the wake of an ionospheric satellite. It should be realized that this decrease in the temperature refers to the thermal motion of the ions along the x-axis only. Since the plasma is collisionless, the temperature of the ions in the flow direction is not changed in the expansion process. Consequently, for large values of (t) the electron temperature may be several orders of magnitude greater than the effective ion temperature. This then reduces the stability of the plasma (i.e., since $T_e \neq T_i$(effective)).

In all the above discussion $\tau = \frac{x}{z}\sqrt{\frac{MV_o^2}{2T}}$ where: V_o = the velocity of the body (which is supersonic), z is the coordinate in the direction of motion of the body ($z < 0$), x is the coordinate in the direction of the normal to the edge of the body and the results are applicable for the region:

$$\left.\begin{aligned} &X \ll R_0 \\ &|z| \cdot (2T/MV_0^2)^{1/2} \ll R_0 \end{aligned}\right\} \qquad (39)$$

A detailed analysis of the stability in the near wake zone was carried out in Section 12 of Gurevich et al. (1969).

For the case of an expansion of a plasma behind a plate (or:rarefied plasma flow behind a plate) the region of stability is shown in Figure A-7. In this figure the results for a plasma with $\beta = 1$ are shown. Ion acoustic waves are unstable in the region above the curve, and the region of instability expands with the increase in β. Note that the vertical and horizontal coordinates in this figure (ρ, t) are defined as:

$$\rho = \frac{x}{R_0} \; ; \; t = \left(\frac{z}{R_0}\right) \Big/ \left(\frac{MV_0^2}{2T_e}\right)^{1/2}$$

where z is the axis parallel to the velocity of the incident plasma flow (flux) and the x-axis is orthogonal to the velocity (V_o) and to the axis of the plate. The plate has a width of $2R_o$ which is infinite in the y-axis direction.

α. Flow of a plasma containing a mixture of ions

The case of a plasma (e.g. the lower ionosphere) having more than one ion species was dealt with by Gurevich et al. (1969) and expanded in Gurevich et al. (1973). Briefly, if we have a plasma with two kinds of ions (e.g. $[O^+]$ and $[H^+]$ with atomic mass units M_1 and M_2 than the following equations should be solved:

$$(u_1-\tau)\frac{\partial g_1}{\partial \tau}-\frac{1}{2}\frac{\partial g_1}{\partial u_1}\frac{d}{d\tau}\left[\ln\left(\int_{-\infty}^{+\infty}g_1 du_1+\sqrt{\frac{M_1}{M_2}}\int_{-\infty}^{+\infty}g_2 du_2\right)\right]=0$$

$$(u_2-\tau)\frac{\partial g_2}{\partial \tau}-\frac{M_1}{2M_2}\frac{\partial g_2}{\partial u_2}\frac{d}{d\tau}\left[\ln\left(\int_{-\infty}^{+\infty}g_1 du_1+\sqrt{\frac{M_1}{M_2}}\int_{-\infty}^{+\infty}g_2 du_2\right)\right]=0 \quad (40)$$

where $u_1 = V_1/\left(\frac{2T_e}{M_1}\right)^{1/2}$; $u_2 = V_2/\left(\frac{2T_e}{M_2}\right)^{1/2}$.

The boundary conditions for $\tau \to -\infty$ are:

$$g_1 = \exp\left(-\beta u_1^2\right)$$

$$g_2 = \alpha \cdot \exp\left(-\beta u_2^2 \cdot \frac{M_1}{M_2}\right) \quad ; \quad \alpha = \frac{N_{20}}{N_{10}} \quad (41)$$

The solution of the system... depend now not only on $\beta = \frac{T_e}{T_i}$, but also on the ratio of the masses $\left(\frac{M_1}{M_2}\right)$ and on the ratio of the initial concentrations $\alpha = \left(\frac{N_{20}}{N_{10}}\right)$. If $M_2 > M_1$ (say; $H(O^+) = 16$ and $M(H^+) = 1$) than at large values of (t) the lighter particles dominate, irrespective of their initial concentrations. Hence, if we assume that $N_2 << N_1$ (which is the case of the terrestrial ionosphere for H < (400 - 500) km) we find that, behind an ionospheric satellite with $\frac{M_2}{M_1} = 16$, the concentration of $[H^+]$ ions is much larger than the concentration of $[O^+]$ even if the $[H^+]$ ions form less than (1 - 10%) of the ions in the undisturbed plasma.

D. About the flow over bodies having a similar cross section to the flow

The question of the flow over bodies having different shapes and cross section was addressed by several papers of Russian group (e.g. Al'pert, 1976; Al'pert et al., 1965; Gurevich et al., 1969). Briefly, they show that based on the law of similarity the pictures of the flow past bodies are similar if the bodies have the same contours in the variables (ρ, t) where: $\rho = \frac{\vec{r}}{R_o}$ and $t = \left[\left(\frac{z}{R_o}\right) \times \left(\frac{2T_e}{MV_o^2}\right)^{1/2}\right] = \left(\frac{z}{R_o}\right)\frac{1}{S}$ where S = ionic Mach number $\equiv \frac{V_o}{V_T(i)}$; $V_T(i)$ = thermal ion velocity.

Note: The laws of similarity found for the rarefied plasma flows (e.g. Gurevich et al., 1969) and analogous to the laws of similarity is supersonic aerodynamics.

In fact in dealing with the case of rarefied plasma flow over a disc of radius R_o it is argued that the disc case is of general significance since it represents the flow over any body of rotation provided that the length of the body (L) is not too large, i.e.,

$$[L/s] \ll R_o \tag{42}$$

and that the results obtained for the disc will be valid for such a body at sufficiently large distances. This is particularly so for flow past a body of rotation with a flat near side.

D. Comments on the influence of the electric field

The influence of the electric field (Gurevich et al., 1969; Al'pert, 1976) is discussed via a comparison with the 'neutral approximation' (where no electric field effects exist).

Note: In Al'pert et al. (1965) the expressions used for the ion densities are in fact those of the "neutral approximations".

For example for the case of flow over a semi-plane the difference between the "neutral approximation" and the calculations of ion distribution (based on the discussion given in this appendix) is shown in Figure A-5. As seen from the figure, the distributions of ions and neutrals are similar for negative and small positive values of $\tau = \varphi/t < 0.5$, in fact they are identical to within 10%. On the other hand in the region of maximum rarefaction ($\varphi = 0$ or large τ) they differ by orders of magnitude. Gurevich et al. (1969) have performed similar comparisons for wakes behind a plate and a cylinder and reached similar conclusions. Furthermore, for the case of a sphere (or a disc) the difference between ions and neutral particles in regions which are not strongly rarefied (e.g. $N \geq 0.2N_o$) the deviation of the distribution of ions from the distribution of neutrals are more significant (see Figure A-8). The role of the electric field increases substantially with the increase of the ratio $[T_e/T_i]$ (see Fig.

A-8, for $\beta = 4$). Another example showing the difference the distribution according to the "neutral approximation" (or: free motion of molecules) and ions in the wake of a plate and a cylinder is given in Figure A-9.

f. About theory-experiment comparisons and the use of the expression $[N/N_o]$ (given in the text)

Gurevich et al. (1969); Gurevich et al. (1973) and Al'pert (1976) have shown results for theory-experiment comparisons. The first two references performed comparisons with in-situ measurements (mainly using results by Samir et al.) and Al'pert (1976) showed comparisons with both in-situ and laboratory measurements.

In this section we will show the degree of agreement obtained via presenting a set of figures.

Figure A-10 shows the degree of agreement between measurements of $I_e^* = f(\theta)$, obtained from the Ariel I (U.K.) satellite and computation by Gurevich et al. (1969) using an expression for flow behind a cylinder.

This expression is formula (54) p. 830 in the above reference. The computation was done for $\beta = 1$ and $b = 3.75$, and is displayed by the solid line. As seen there is good agreement for $\theta \lesssim 120°$ only.

Figure A-11 shows the degree of agreement between $I^*_e = f(\theta)$ at a distance of $5R_o$ from the center of the Ariel I satellite, as measured by the boom mounted electron probe (guarded plane probe) and between the Gurevich et al. (1969), Al'pert (1976) computations given by the solid line. Here as in Figure A-10 the computation was done for $\beta = 1$; $b = 3.75$ using the expression for the "neutral approximation". Although the measurements were for the current ratios $I^*_e = [I_e/I_o]$ (which is the ordinate of the figures) and the computations for $N^* = [\frac{N}{N_o}]$ it was assumed that: $[I_e/I_o] \simeq [N_e/N_o]$. Of particular interest in Figure A-11 is the fact that the "neutral approximations" (at: $Z = 5R_o$ from the center of the satellite) predicts satisfactorily the degree of electron current depletion at the maximum rarefaction ($\rho = 0$; large τ) on the wake axis.

Figure A-12 shows the comparison between $I^*_e = f(\theta)$ measured by an electron probe flush mounted on the surface of the Explorer 31 satellite and the Gurevich et al. (1969) computations.

Note: The probe on the Explorer 31 was similar to that on the Ariel I satellite. The result shown is similar to that shown in Figure A-10. An the expression used in the computation is identical to that used for Figure A-10.

Figure A-13 shows a comparison of some Explorer 31 results with results of computations using expression (1) given in text of the paper i.e., the expression:

$$\frac{N(\theta)}{N_0} = n(O^+)\left[\frac{1+erf\left(b(O^+)\cdot\cos\varphi_0\cos\theta\right)}{1+erf\left(b(O^+)\cdot\cos\varphi_0\right)}\right] + n(H^+)\left[\frac{1+erf\left(b(H^+)\cdot\cos\varphi_0\cos\theta\right)}{1+erf\left(b(H^+)\cos\varphi_0\right)}\right]$$

As seen from this figure the agreement between theory and experiment is very reasonable.

If $[H^+]$ is the major ionic constituent for altitudes above (500 - 600 km) in the terrestrial ionosphere than the effect of the electric field on the motion of the ions is small (since the ionic Mach number $S(H^+)$ is small) and in the boundary of the wake the field can be ignored. The angle (φ_o) in expression (1) characterizes the wake boundary as seen by the probe situated at $_o$ on the satellite. For the comparisons shown in Figure A-13, the angle $\varphi_o = 45°$.

Another conclusion (or: recommendation) of Gurevich et al. (1969) is that when the relative value of $[H^+]$ in the plasma exceeds about 30%, expression (1) can be applied.

Figure A-14 shows the dependence of $[\frac{J(\theta = 180°)}{Jo}]$ on $n_{H+}[\ N(H^+)/N_o(\text{total})]$ in the range $0 < n_{H+} < 0.75$ (after Gurevich et al., 1969), in the quasi-neutral region. The solid line shows the results of the calculation using expression (1) for T_e = constant, the dotted line shows is essentially the same but taking account of the variation in T_e and the points are Explorer 31 data points (after Samir and Wrenn, 1969).

In Gurevich et al. (1973) it was shown that in a plasma which expands into a vacuum a portion of the ions is accelerated and the energy they may obtain by the process of acceleration can be of the order of $(10^2 - 10^3)\ T_e$. In that publication the excitation of waves (e.g. ion-acoustic waves) is also investigated.

The treatment is that of a plasma having <u>two ionic species</u> i.e., $[H^+]$ and $[O^+]$. Based on the computation given in this paper the behavior of Figure A-14 was replotted and as can be seen in Figure A-15 there is a better agreement between theory and experiment. In Figure A-15 the dotted line represents the calculation using the expression:

$$N(\tau) = \frac{1}{2} N(O^+) \left[1 + \operatorname{erf}\left[\left(\frac{M_2}{M_1} \right)^{1/2} \cdot \tau \right] \right] + \frac{1}{2} N(H^+) \left[1 + \operatorname{erf}(\tau) \right] \qquad (43)$$

i.e., essentially using expression (1). As is seen from this figure the solid line depicts a better agreement with experiment for $n_{H^+} \geq 0.4$.

<u>In conclusion:</u> It appears that for specific cases of practical interest in the terrestrial ionosphere and in planetary ionospheres semi-analytical expressions for the distribution of particles around a body may be adequate and there may be no practical need to seek very elaborate and costly numerical codes.

This conclusion may also be of practical interest to spacecraft-charging.

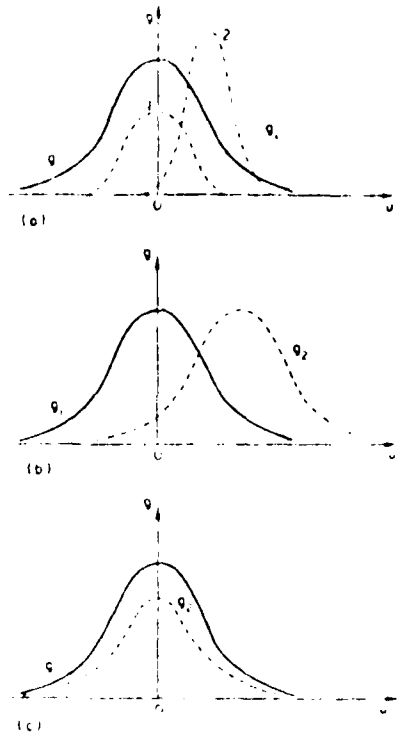

Fig. A-1. Classification of initial discontinuities. Different relations between the boundary distribution functions g_1 and g_2: (a) $T_1 = T_2$; (b) $T_1 = T_2$, $v_0 \neq 0$; (c) $T_1 = T_2$, $v_0 = 0$, $N_1 > N_2$.

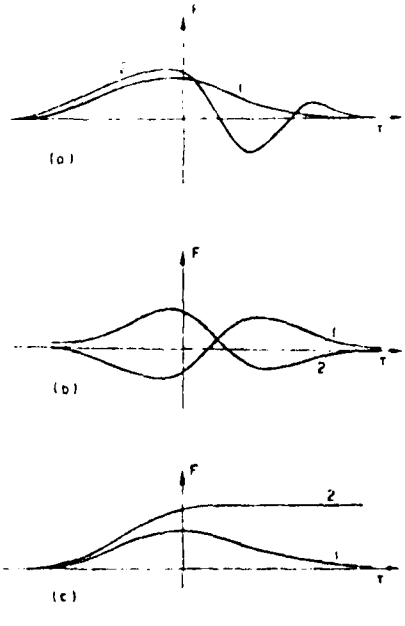

Fig. A-2. Non-dimensional force $F(\tau)$ for the same cases as in Fig. 1. The sign of the velocity v is different in the curves 1 and 2 of case (b). Curve 2 of case (c) corresponds to the free expansion of plasma into vacuum: $N_2 = 0$.

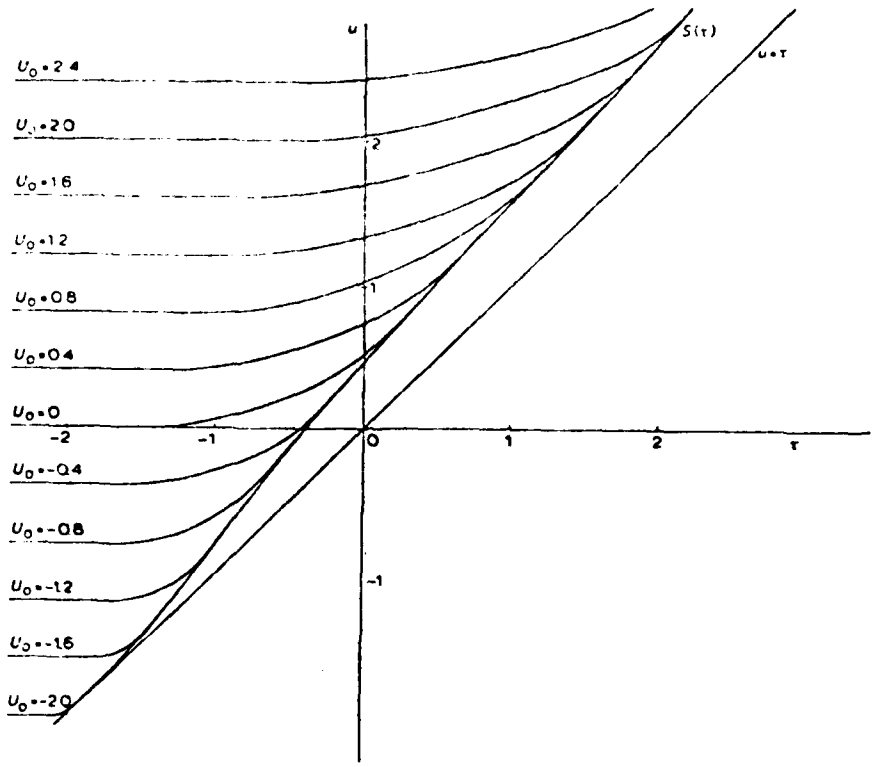

Fig. A-3. Flow past a semi-plane. The behaviour of characteristics in (u, τ) plane for

$$\beta = \frac{T_e}{T_i} = 1, \qquad u = v/\sqrt{2T_e/M}, \qquad \tau = \frac{Q}{t_*} = \sqrt{\frac{M\bar{V}_0^2}{2\bar{T}_e}}\,\frac{x}{z}.$$

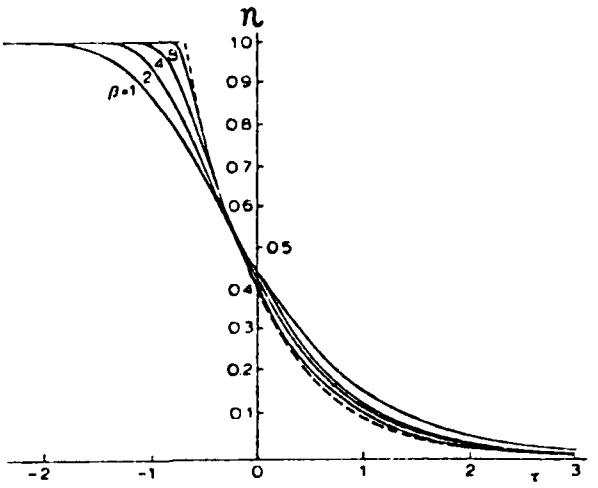

Fig. A–4. Flow past a semi-plane. The dependence of concentration

$$n = N/N_0 \quad \text{on} \quad \tau = \frac{\varrho}{l} = \sqrt{\frac{MV_0^2}{2T_e}}\,\frac{x}{z}$$

for different values of $\beta = T_e/T_i$. The dotted line is obtained in the case of isothermal hydrodynamics, which corresponds to the limit $\beta \to \infty$.

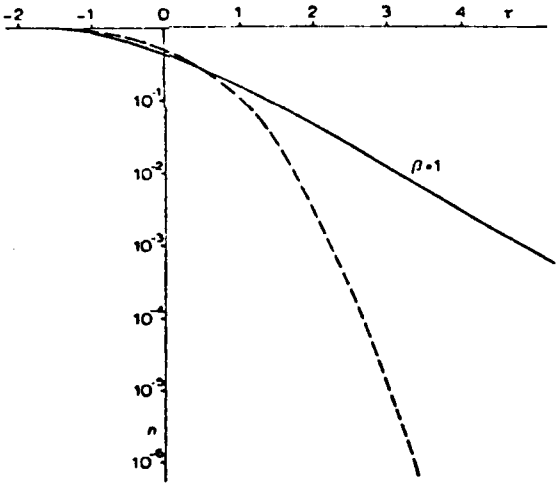

Fig. A–5. The same on a logarithmic scale ($\beta = 1$). The dotted line is obtained for free motion of molecules, which corresponds to the limit $\beta \to 0$ ('neutral approximation'.)

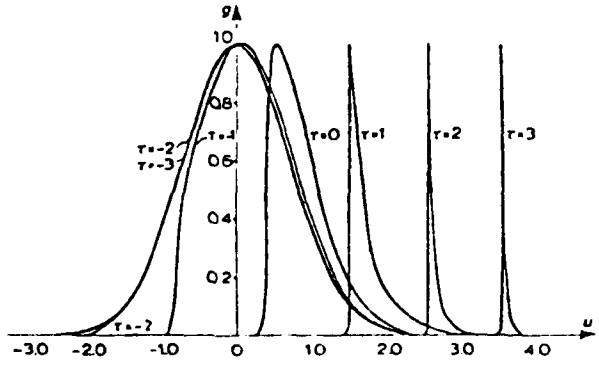

Fig. A-6. Flow past a semi-plane. The distribution function $g(u)$ for different values of τ.

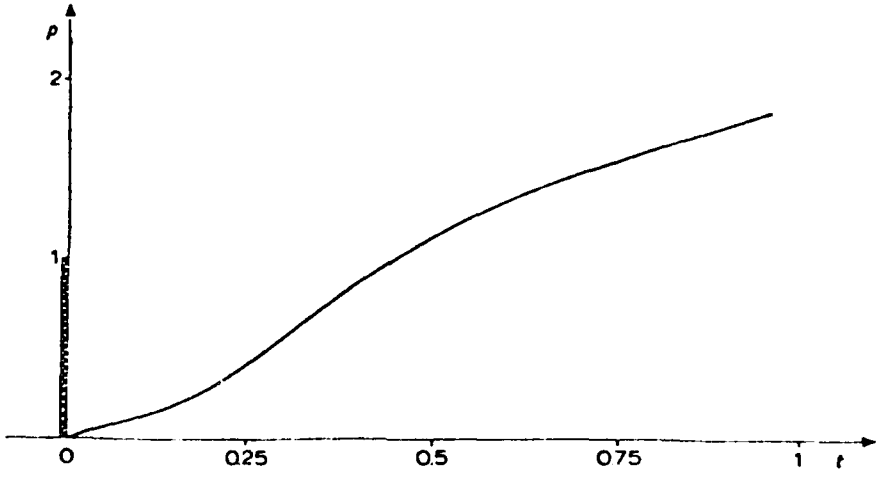

Fig. A-7. The boundary of the region of instability for flow past a plate ($\beta = 1$). Ion acoustic waves are unstable in the region above the curve.

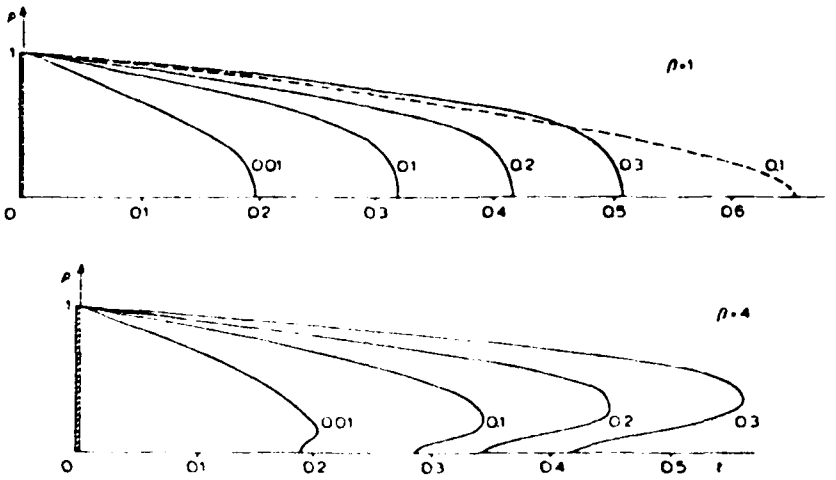

Fig. A-8. The surfaces of constant concentration of ions for flow past a disc (a) $\beta = T_e/T_i = 1$, (b) $\beta = 4$. The dotted line corresponds to free motion of molecules.

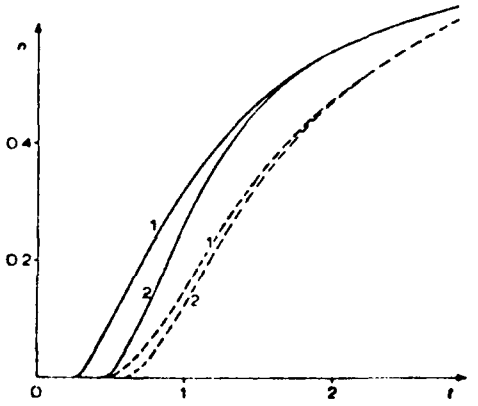

Fig. A-9. The dependence of

$$n = \frac{N}{N_0} \quad \text{on} \quad t = \frac{z}{R_0}\sqrt{\frac{2T_e}{MV_0^2}} \quad \text{for} \quad \beta = 1$$

along the $\varrho = 0$ axis behind a plate (curve 1) and behind a cylinder (curve 2, $b = \sqrt{\frac{MV_0^2}{2T_e}} = 2.5$).

The dotted lines show the same quantities for free motion of molecules.

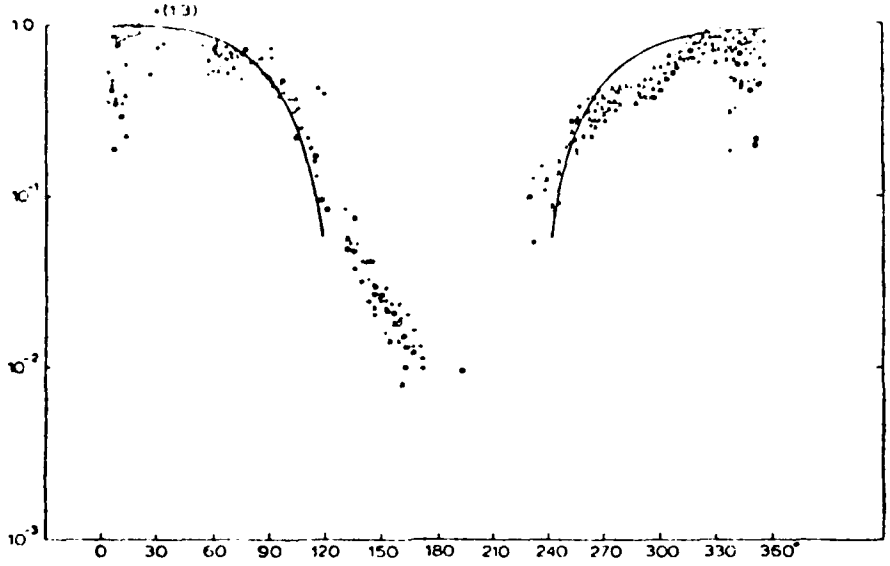

Fig. A-10.

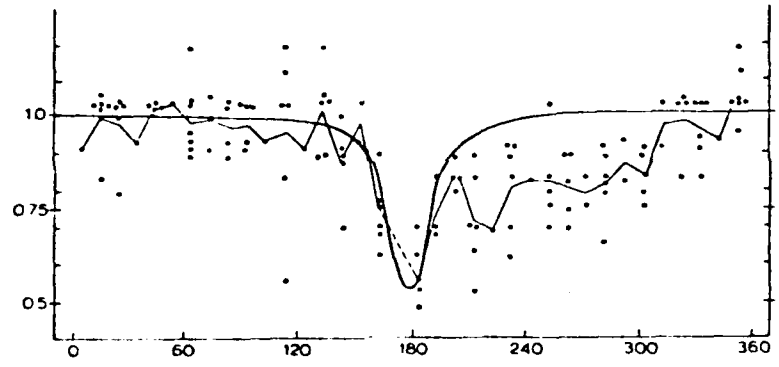

Fig. A-11.

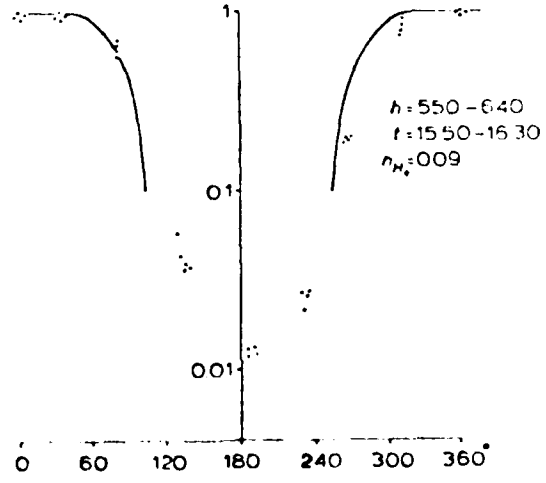

Fig. A-12.

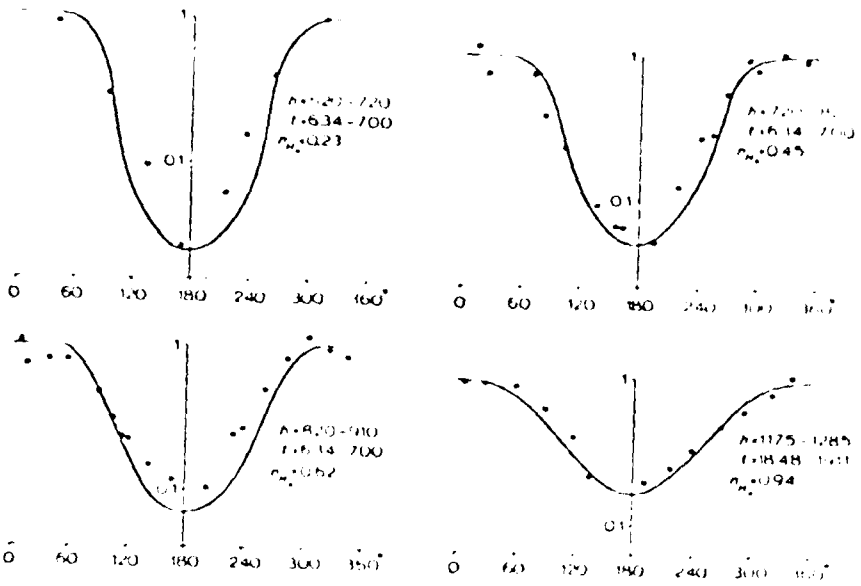

Fig. A-13.

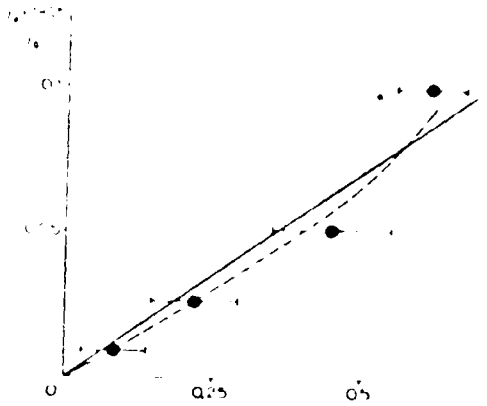

Fig. A-14.

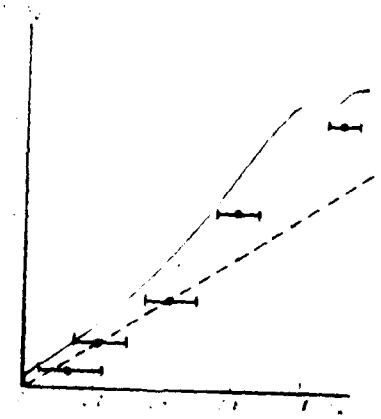

Fig. A-15.